

PAM: Processing Across Memory Hierarchy for Efficient KV-centric LLM Serving System

Lian Liu*

Shixin Zhao*

Institute of Computing Technology,
CAS, University of Chinese Academy
of Sciences
Beijing, China

liulian211,zhaoshixin18@mails.ucas.ac.cn

Mengdi Wang

State Key Lab of Processors, Institute
of Computing Technology, Chinese
Academy of Sciences
Beijing, China
wangmengdi@ict.ac.cn

Yutian Zhou

Institute of Computing Technology,
Chinese Academy of Sciences,
University of Chinese Academy of
Sciences
Beijing, China
zhouyutian23s@ict.ac.cn

Yintao He

Institute of Computing Technology,
Chinese Academy of Sciences,
University of Chinese Academy of
Sciences
Beijing, China
heyintao19z@ict.ac.cn

Ying Wang†

State Key Lab of Processors, Institute
of Computing Technology, Chinese
Academy of Sciences
Beijing, China
wangying2009@ict.ac.cn

Abstract

The widespread adoption of Large Language Models (LLMs) has exponentially increased the demand for efficient serving systems. With growing requests and context lengths, key-value (KV)-related operations, including attention computation and KV cache storage, have emerged as critical bottlenecks. They require massive memory bandwidth and capacity. Unfortunately, existing LLM serving systems, optimized for compute-bound workloads, fail to handle these memory-intensive operations effectively. Even with Processing-In-Memory (PIM) technology, current single-level memory designs cannot simultaneously satisfy the bandwidth and capacity requirements, particularly in cost-sensitive cloud environments.

To address these challenges, we propose Processing Across Memory (PAM), a KV-centric LLM serving system that coordinates heterogeneous PIM-enabled memory devices within a hierarchical architecture. PAM introduces a novel computing paradigm to balance high memory bandwidth with scalable capacity. First, PAM exploits the inherent context locality in KV access patterns to intelligently distribute KV tokens across the memory hierarchy with near-data computing capability. Second, to further exploit context locality, it introduces the PAMattention algorithm, enabling fine-grained parallel attention computation across heterogeneous PIM devices. Finally, PAM incorporates an intra-device KV mapping, inter-device KV migration interface, and an inter-device online KV scheduling algorithm to dynamically balance computational workloads and reduce data transfer overhead. PAM adopts a full-stack design that orchestrates diverse PIM devices as a unified, hierarchical system to meet both bandwidth and capacity demands. By addressing both bandwidth and capacity demands simultaneously, PAM significantly enhances the efficiency and scalability of LLM serving systems, paving the way for cost-effective, high-performance solutions in the era of large-scale AI.

Yinhe Han

State Key Lab of Processors, Institute
of Computing Technology, Chinese
Academy of Sciences
Beijing, China
yinhes@ict.ac.cn

1 Introduction

Large Language Models (LLMs) [2, 107, 108] have emerged as a transformative force in generative AI, revolutionizing applications such as chatbots [14, 15, 28], search engines [40, 119], and automated customer service [83, 87]. The rapid adoption of LLM-based solutions has led to an exponential increase in demand for efficient serving systems, with modern deployments handling millions of requests daily [48]. This surge in demand has driven the development of various LLM serving systems [3, 45, 56, 60, 61, 82, 85, 126, 138], which aim to optimize serving performance in increasingly resource-intensive scenarios.

Despite these advancements, existing solutions are constrained by two major limitations. First, many systems rely on large-scale, high-performance hardware infrastructures, such as tightly interconnected GPU clusters and expensive High Bandwidth Memory (HBM), to improve processing capability. While effective, these approaches often come with exorbitant costs and energy consumption, making them impractical for cost-sensitive environments. Second, these systems are predominantly compute-centric, prioritizing the optimization of compute-bound operations. However, key-value (KV)-related operations, including attention computation and KV cache storage, constitute the primary bottleneck in LLM serving systems. Attention computation, which generally accounts for over 80% of runtime, is inherently bandwidth-bound as it requires loading all previously generated KV (referred to as KV-tokens in this paper) to generate each new token [110]. KV cache, storing pre-computed key-value vectors to avoid redundant computations, can occupy over 95% of the total memory capacity [32, 45, 56]. Together, these operations demand both high memory bandwidth and vast memory capacity, creating a fundamental mismatch with compute-optimized designs.

Recent studies have explored various hardware [78, 79, 81, 116, 139] and software [4, 8, 37, 102] techniques to alleviate these bottlenecks. Among these, Processing-In-Memory (PIM) architectures¹ [44,

*Both authors contributed equally to this research.

†Corresponding author.

¹For simplicity, DRAM-based and Flash-based PIM/Near Data Processing are collectively referred to as PIM in this paper.

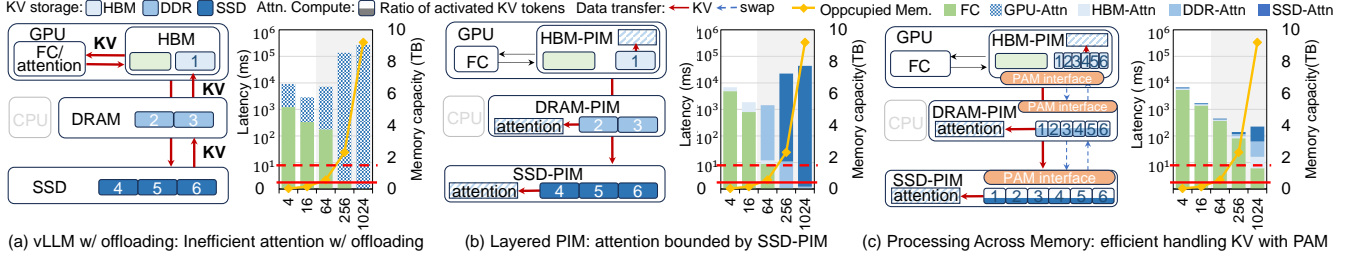


Figure 1: Illustration of (a) vLLM with offloading; (b) Layered PIM; and (c) PAM. System illustration is on the left side of each subfigure and the performance breakdown is on the right side of each subfigure. The x-axis of the histogram is batch size. The red solid line indicates the maximum capacity of HBM and the red dotted line indicates the maximum DDR capacity.

[47, 52, 69, 92, 116] have gained prominence. These architectures integrate computational units directly into memory devices, providing increased bandwidth. Systems such as AttAcc! [79], which leverage HBM-PIM [51], achieve up to 9x higher aggregated memory bandwidth than NVIDIA DGX A100 [74], significantly improving attention computations performance. However, the high cost of large-scale HBM-PIM deployments renders them impractical for scaling KV cache capacity to handle millions of requests. Alternatively, as shown in Figure 1(a), offloading-based approaches [33, 54, 95, 97, 121] transfer KV data to inexpensive host memory (e.g., DDR) or non-volatile memory (e.g., SSDs) to expand memory capacity. While cost-effective, these systems suffer from limited bandwidth, as SSDs typically offer less than 5 GB/s compared to the 2 TB/s bandwidth of GPUs with HBM. While these approaches have shown promise, they fail to simultaneously address the dual demands for bandwidth and capacity.

Instead of relying on isolated memory levels or compute-centric optimizations, we argue for a hierarchically coordinated approach that leverages the strengths of heterogeneous memory devices. A straightforward solution is to enable in-situ processing in the current hierarchical memory system, i.e. layered processing-in-memory (L-PIM) system as we defined. As shown in Figure 1(b), L-PIM distributes KV tokens across HBM, DDR, and SSD, providing large capacity and enhanced bandwidth [25, 62, 90, 111, 118]. However, simply putting PIM devices together shows that a new bottleneck emerges in attention computation, e.g. SSDs (SSD-Attn), as memory usage increases. This bottleneck arises from a mismatch between the memory access intensity and the provided bandwidth of different memory devices in the L-PIM system. Specifically, since all KV tokens participate in attention computation, the lowest-level memory, such as SSDs, which store the majority of KV tokens, endures the highest frequency of data accesses. However, their limited bandwidth poses significant challenges for efficient data retrieval, leading to substantial performance degradation. For example, SSD-PIM solutions [35, 55, 57, 65] provide a bandwidth of less than 100 GB/s—merely 5% of the bandwidth offered by HBM-PIM, highlighting the stark disparity in performance capabilities across the memory hierarchy.

This limitation underscores the need for a fundamentally new approach that goes beyond simply combining heterogeneous PIM devices. Processing Across Memory (PAM) addresses this challenge by coordinating KV-related operations across the memory hierarchy in a context-aware, algorithmically optimized manner, as illustrated

in Figure 1(c). PAM adopts a full-stack design to align algorithms, architectures, and system management with the unique demands of KV-related operations. Leveraging multi-step strategies, PAM overcomes the inefficiencies that limit hierarchical PIM systems.

First, PAM identifies and exploits the **context locality** inherent in KV caches. Recent studies reveal that attention mechanisms are inherently sparse [22, 54, 86, 123, 129], requiring only a subset of KV tokens for subsequent token generation. By analyzing this sparsity, PAM uncovers a strong context locality pattern: KV tokens accessed in recent decoding steps are more likely to be reused in adjacent token generations (§3.2). This insight enables PAM to efficiently distribute KV tokens across the memory hierarchy according to their access patterns. For example, frequently accessed tokens are allocated to HBM, optimizing data placement to leverage the memory hierarchy effectively.

Second, the context locality necessities partitioning KV tokens onto heterogeneous PIM devices, which cannot be achieved through existing request-level solutions [8, 31, 79, 126]. PAM achieves fine-grained distributed attention orchestration by introducing the PA-Mattention algorithm. Specifically, PAMattention achieves token-wise parallelization across hierarchical PIM devices by dividing each attention computation into local and global stages (§5), enabling each PIM device to process its allocated KV tokens locally while contributing to the overall computation in parallel. In addition, the distributed attention model introduces additional reduction requirements, which PAM addresses with hierarchical reduction units that efficiently handle intra- and inter-device reductions with minimal overhead. This architecture ensures seamless collaboration across heterogeneous PIM devices, delivering scalable performance for memory-intensive attention operations.

Third, PAM implements a KV-centric management strategy to harness the potential of context locality and balance workloads across the memory hierarchy (§6). The management mechanism comprises three components, including intra-device KV mapping, PAM interface, and inter-device KV scheduling. First, the intra-device KV mapping employs a PIM-aware address mapping mechanism to balance workloads and maximize processing capabilities within each PIM device. Second, since the data addressing and layouting mechanism for each PIM device is quite different, we introduce a novel PAM interface to facilitate efficient data layout transformations during KV token transfers across memory layers, minimizing transfer overhead. Finally, based on real-time changing patterns of KV accessing, we propose a novel inter-device KV

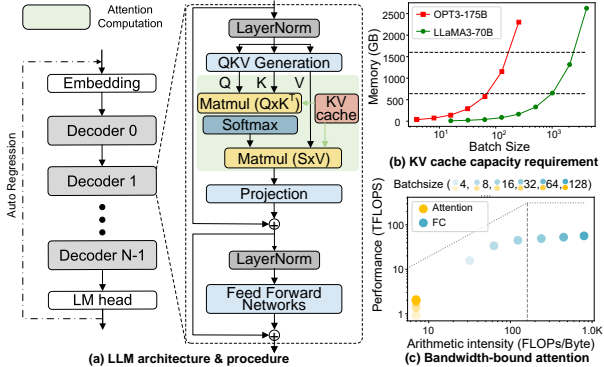


Figure 2: (a) LLM architecture. (b) The requirements of LLM serving. (c) Roofline model of attention computation.

scheduling strategy to achieve dynamic load balancing across heterogeneous PIM devices with minimal data transfer overhead.

Figure 1(a)-(c) visualizes the offloading system designs of L-PIM and PAM, highlighting how PAM effectively addresses key bottlenecks in LLM serving. Performance breakdowns illustrate that PAM delivers significant improvements in meeting modern LLM deployment demands. In general, we make the following contributions.

- We present PAM, a scalable LLM serving system that unifies heterogeneous PIM tiers, including HBM-PIM, DRAM-PIM, and SSD-PIM, into a hierarchical memory-compute architecture. Instead of treating each PIM tier in isolation, PAM adopts a top-down co-design approach that orchestrates execution across all tiers. By aligning KV-related operations with tiered architecture, PAM balances bandwidth and capacity demands while maintaining cost efficiency.
- To reduce inter-tier data movement and exploit hierarchical PIM compute capabilities, we propose PAMattention—a hardware-software co-designed attention algorithm optimized for tiered memory. PAMattention enables fine-grained, token-level parallelism by performing in-situ softmax and embedding dedicated reduction units in each memory tier, reducing communication to achieve efficient attention across heterogeneous PIM tiers.
- PAM exploits intrinsic context locality to coordinate cross-tier data placement and movement through a suite of KV management mechanisms. Specifically, PAM utilizes intra-device KV mapping to maximize processing parallelism in each PIM module, while providing a unified inter-device PAM interface and scheduling strategy to minimize the migration of KV tokens across the memory hierarchy.
- Compared to the industry-standard DGX-H100 based vLLM [45] serving system, PAM achieves an average **12.88 \times** and **26.41 \times** performance improvement for conversation and long-context processing, respectively, showcasing its significant advantages in throughput and cost-effectiveness for LLM serving.

2 Background

2.1 LLM Architecture & Inference

2.1.1 *LLM Architecture.* As shown in Figure 2(a), generative LLMs are constructed with multi-layered transformer blocks [110]. There are two major operators in a transformer block: fully connected (FC)

in blue and attention in green. These two components dominate the computational and memory overhead during inference, making their optimization critical for efficient performance.

2.1.2 *LLM Inference Procedure.* LLM inference operates in two phases: prefill and decoding. In the prefill phase, the model processes m user-input tokens in parallel to generate the first new token x_{m+1} , leveraging the parallelism of modern hardware such as NVIDIA H100 GPUs [76]. In the decoding phase, LLM leverages an autoregressive manner, wherein each generated output token serves as the input for generating the next token. Furthermore, to avoid redundant computations, key and value (KV) vectors of previously generated tokens, known as KV cache, are stored to be reused in subsequent tokens. For example, LLM takes the t -th token as input and utilizes the KV cache of preceding tokens $1 \sim t$ to generate the $(t + 1)$ -th token.

2.2 LLM Serving Requirements

Efficient LLM serving often involves batching multiple user requests to maximize hardware utilization. However, handling batched KV-related operations introduces significant demands for both memory capacity and bandwidth.

2.2.1 *Large Capacity for KV Cache Storage.* The KV cache size grows linearly with batch size, creating significant storage pressure. For instance, processing 256 OPT-175B requests with 2048-token contexts requires approximately 2304 GB of KV cache, which far exceeds the capacity of platforms like DGX-H100 [75]. This storage bottleneck severely limits large-scale deployment feasibility.

2.2.2 *High Bandwidth for Attention Computation.* As illustrated in Figure 2(c), attention operations are inherently memory bandwidth-bound as the arithmetic intensity of attention does not scale with various batch size [79, 92]. To make it worse, the loading cost of KV cache grows linearly with the context length since the attention operator requires all pre-generated KV tokens during decoding.

2.3 Optimizations on KV-related Operations

To address the challenges of KV-related operations, researchers have developed solutions spanning algorithmic, software, and hardware innovations.

2.3.1 *KV Sparsity.* Due to the linguistic distribution properties of natural language [5, 89], attention is inherently sparse [22]. Researchers have explored various sparsity strategies to optimize KV usage, which can be categorized into two types: eviction-based sparsity and retrieval-based sparsity. Eviction-based KV sparsity strategies [11, 26, 36, 96, 117, 133] store only a subset of important tokens by evaluating token significance during KV cache generation and evicting less critical ones. While significantly reducing KV cache storage overhead, these methods often degrade model accuracy by permanently discarding tokens that may become important in subsequent decoding steps. In contrast, retrieval-based sparsity strategies [22, 54, 86, 99, 123] store the entire KV cache but selectively load the most relevant tokens during attention computation. However, retrieval-based methods do not reduce storage footprint, as they still cache the full KV set.

2.3.2 PIM-based Acceleration. Processing-In-Memory (PIM) architectures address the bandwidth demands of attention computations by integrating computational capabilities directly into memory devices [42, 44, 52, 58, 139]. Two common design approaches are: near-bank/plane and on-controller designs. In near-bank PIM designs, processing units are placed close to the memory banks. This design enables operations to be performed directly using data read from the row buffers, fully exploiting the internal bandwidth of multiple memory banks to process bandwidth-bound attention operators. For example, AttAcc! [79] leverages the high aggregate memory bandwidth of HBM-PIM [51] for efficient attention computations. However, near-bank PIM design cannot achieve efficient data communication across different banks [27, 72, 106].

On-controller designs [58, 140] centralize computation within the memory controller, enabling operations such as reductions without data movement. While this improves efficiency in certain cases, it provides lower bandwidth than near-bank PIM approaches.

2.3.3 Memory Management. To address the significant storage requirements of KV caches, memory management strategies have been developed to efficiently utilize fragmented resources across heterogeneous devices [13, 29, 66, 71, 84, 95, 120]. For example, vLLM introduces a paged attention mechanism that maps KV caches into multiple blocks within GPU memory, reducing fragmentation [45]. However, GPU memory constraints still limit scalability. To address this issue, offloading-based strategies provide additional capacity by transferring portions of the KV cache to CPU memory or SSDs [34, 54, 95]. For example, DeepSpeed-Inference [8] offloads KV cache to host memory to expand available capacity. This approach effectively increases the available serving capacity. However, such systems must transfer KV caches back to GPU memory for computation, creating bottlenecks due to the limited bandwidth of interconnects like PCIe that bridge heterogeneous memory devices, making it challenging for offloading-based heterogeneous systems to achieve efficient LLM serving.

3 Motivation & Challenges

3.1 Limitations of Layered PIM

Existing approaches, including offloading-based strategies [33, 54, 95, 97, 121] and PIM architectures within single-level memory device [30, 78, 92, 116, 127, 139], fail to address the dual challenges of massive memory capacity and high bandwidth required for efficient LLM serving. L-PIM systems offers a promising alternative [6, 8, 18, 21, 25, 29, 115]. However, as shown in Figure 1(b), L-PIM systems do not significantly improve LLM serving efficiency.

The main limitation arises from the mismatch between KV-related operation patterns and the processing capabilities of L-PIM systems. Attention computation requires loading all pre-generated KV tokens when generating a new token. Due to the large capacity of KV caches, most tokens are offloaded to cost-effective memory like SSDs. This results in an inherent bottleneck: the memory device storing most KV tokens experiences the highest access pressure, yet devices with the largest storage capacity offer the lowest memory bandwidth, far below the requirements of KV-related operations [35, 55, 57, 65]. This inefficiency arises as the traditional

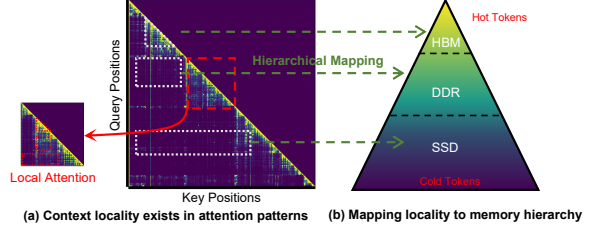


Figure 3: Exploiting context locality to achieve hierarchy memory processing.

memory hierarchy is optimized for exploiting data distribution locality, which is absent in KV operations. KV tokens used in attention computation are treated uniformly, regardless of their relevance or locality. This leads to imbalanced memory access and underutilization of bandwidth across the hierarchy, preventing L-PIM systems from realizing their theoretical performance potential.

3.2 Context Locality

Fortunately, we observed that existing retrieval-based KV sparsity patterns exhibit strong **context locality**, where the same KV tokens are frequently accessed within a short period during decoding. For instance, if a KV token i is accessed at decoding step j , it is highly likely to be accessed again at step $j + 1$. This arises from the semantic properties of natural language, where adjacent tokens are often semantically linked, maintaining tight relationships with specific KV tokens [59, 93, 132]. As illustrated in Figure 3(a), we analyzed the attention pattern of layer-12 in LLaMA2-7B [108]. The most relevant KV tokens are denoted in yellow, while the KV tokens in dark blue are useless. The results indicate that a small subset of KV tokens plays a key role in accuracy, while the rest are sporadically activated. Furthermore, these critical KV tokens tend to cluster around the current token, reflecting their local relevance and semantic proximity.

This context locality motivates us to leverage it within the memory hierarchy, to process KV-related operations across the memory hierarchy. As illustrated in Figure 3(b), we leverage the activated frequency to guide the mapping of KV tokens to different layers of the PIM hierarchy. It enables collaborative attention computation across PIM devices, optimizing both efficiency and performance.

3.3 Challenges

To realize the proposed Processing-Across-Memory (PAM) paradigm and fully exploit the benefits of context locality, the following key challenges must be addressed:

3.3.1 C1: Inefficient Attention Computation within Heterogeneous PIM Devices. As shown in Figure 2(a), attention computation involves three main kernels: two matrix multiplications (matmul) interleaved with a softmax operation. Unlike matmul, which benefits from efficient tiling [94, 137], the all-to-all nature of softmax complicates distributed execution. While KV tokens can be mapped to heterogeneous devices based on activation frequencies, and tiling can optimize the matmul $Q \times K^T$ within each device, softmax requires gathering all outputs onto a single device. The results must then be redistributed for the matmul $S \times V$, incurring significant

overhead due to limited inter-device bandwidth. Minimizing data movement while maintaining computational efficiency is critical.

3.3.2 C2: Dynamic Distribution of Activated KV Tokens. Although context locality exists, the distribution of activated KV tokens evolves dynamically during decoding. As shown in Figure 3(a), their importance shifts over time, influenced by the changing context of token generation. A static KV mapping results in imbalanced memory access, with some devices overloaded while others remain underutilized. To mitigate this, an online scheduling mechanism is needed to predict KV token importance and dynamically redistribute them across the memory hierarchy.

4 PAM: System Overview

We present PAM, an efficient KV-centric LLM serving system that introduces the novel Processing-Across-Memory paradigm to address the challenges mentioned above. Figure 4 illustrates the overview of PAM system, which comprises three core components: a tiered memory hierarchy with PIM capabilities, a centralized system manager, and a heterogeneous processing coordination framework.

4.1 System Architecture

As presented in Figure 4(a), PAM system builds upon modern LLM serving platforms such as DGX-H100 [75], employing high-bandwidth interconnects (NVLink/CXL) between multiple PAM instances. Each instance integrates CPU resources with NPU (e.g., GPUs [73, 76], TPUs [38, 39]) through a multi-tier PIM-enabled memory hierarchy spanning HBM, DDR, and SSD. NPUs connect to HBM via 2.5D packaging, while CPUs interface with DDR and SSD through standard memory buses and PCIe/NVMe, respectively.

PAM innovatively introduces a tiered PIM design combining HBM-PIM, DDR-PIM, and SSD-PIM to accelerate memory-intensive KV-related operations. HBM-PIM and DDR-PIM adopt near-bank processing units (PUs) to exploit DRAM bandwidth, each tier equipped with dedicated reduction units (RUs) for efficient aggregation of variable-length attention (details in §5.2). SSD-PIM employs controller-level PU/RU designs to parallelize attention across flash dies. To support cross-tier access across heterogeneous layouts, each PIM device integrates a PAM interface (see §6.2) to facilitate efficient data transformation and transfer.

While Figure 4 depicts a single-node configuration, PAM seamlessly scales to multi-node deployments. Following strategies in existing large-scale serving systems [85, 114], the system achieves this through RDMA networking (8×400 Gbps interconnects). It also supports hybrid tensor/pipeline parallelism for efficient serving. §7.6 shows near-linear scaling across instances and nodes.

4.2 System Manager

As illustrated in Figure 4(b), PAM incorporates a dedicated System Manager that orchestrates: (1) a compiler framework, (2) Memory and storage space management, and (3) Cross-tier execution scheduling for efficient LLM serving. This management stack is built upon the application level without OS modification.

4.2.1 Compiler Framework. The PAM compiler serves as the system’s frontend, ingesting LLM model specifications (in ONNX format [68]) alongside hardware configuration to produce an executable inference workflow. It performs operator graph parsing, tile sizing, and instruction scheduling to optimize resource usage. Attention operators are compiled into tiered-PIM instructions, while non-memory-bound operators are mapped to NPU kernels. In addition, the compiler performs offline weight layout transformation, to ensure high-throughput access to weights stored in PIM devices and that weight fetching aligns with NPU execution needs.

4.2.2 Memory/Storage Space Management. Aligned with commercial PIM practices [23, 51, 64], PAM manages all PIM-enabled memories (HBM-/DDR-/SSD-PIM) through physical address control, bypassing OS-level abstractions like virtual memory, page faults, or caching. PAM organizes three main types of data: KV cache, model weights, and intermediate activations. For KV cache, PAM adopts PagedAttention [45], using a block table to record the physical locations of KV tokens (see §6.1). To preserve full compute locality within PIM devices, PAM disables address hashing, similar to techniques used in commercial implementations [23, 52]. While this limits CPU/NPU direct access efficiency, separate data placement strategies are used to mitigate the impact. Following Attacc! [79], intermediate activations are mapped directly to memory buffers across tiers, avoiding interference from address hashing. For large-size weights, PAM applies the compile-time layout transformation strategy as in UM-PIM [135] to ensure high-bandwidth utility. The host CPU manages both control flow and the KV block table. Evaluation shows that this management requires less than 4GB per node, so PAM reserves an 8GB region on host memory—comparable to practices in UPMEM and HBM-PIM deployments.

4.2.3 Processing Scheduler. PAM maintains a request pool for incoming queries and schedules execution at runtime. The scheduler prioritizes prefill stages, following vLLM’s policy [46], and manages PAMattention computing and KV token placement across tiered-PIMs to optimize locality and computation (details in §5.1 and §6.3). Each KV token is tagged with an importance factor, stored alongside the block table to guide runtime scheduling.

4.3 Processing Workflow

PAM orchestrates NPUs for compute-intensive tasks and delegates memory-bound operations to tiered PIM modules for efficient end-to-end inference. As shown in Figure 4(c), execution proceeds in two phases. During prefill, NPUs run all operators [82, 138] while distributing KV cache across memory tiers. In decoding, the host offloads QKV generation to NPUs, then transfers the resulting Q, K, and V vectors to tiered PIM modules. The host triggers local attention computations on each PIM tier, with partial results aggregated in HBM-PIM, where reduction units are used to complete the full attention computation (see §5). The attention output is returned to NPUs for output projection and FFN layers. Meanwhile, the scheduler dynamically adjusts token placement across tiers.

5 PAMattention: Attention across Memory

The challenge outlined in §3.3.1 demonstrates that attention computation across memory tiers incurs substantial data movement

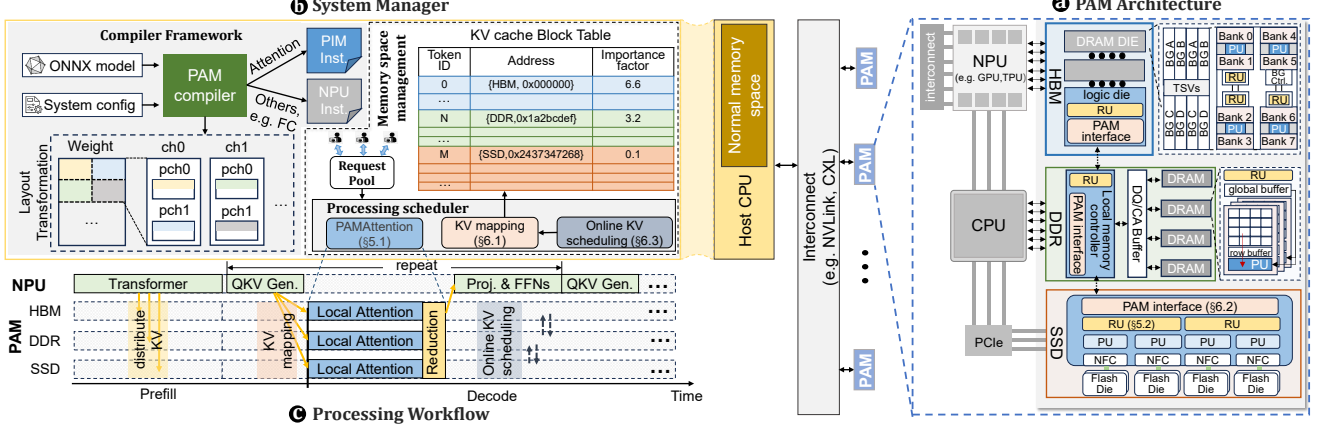


Figure 4: Overview of the proposed KV-centric LLM serving system, PAM.

overhead despite KV sparsity and context locality. Our PAMattention solution introduces in situ *online softmax* for fine-grained token-wise parallelism within each PIM device, dramatically reducing inter-tier transfers. This section details both the algorithm (§5.1) and its associated architectural implementation (§5.2).

5.1 PAMattention Algorithm

5.1.1 Tiling for Softmax. While kernel fusion [10, 70, 136, 137] reduces data movement, attention computations resist fusion due to softmax's all-to-all dependencies. To overcome this, we adopt an equivalent transformation method, enabling softmax tiling [21, 94, 109] with online scaling. Specifically, the softmax computation for a vector $x \in \mathbb{R}^{1 \times d}$ is defined as:

$$m(x) := \max_i x_i, \quad f(x) := [e^{x_1 - m(x)}, \dots, e^{x_d - m(x)}], \quad (1)$$

$$\ell(x) := \sum_i f(x)_i, \quad \text{softmax}(x) := \frac{f(x)}{\ell(x)}. \quad (2)$$

By tiling the input vector into sub-vectors $x = [x^{(1)}, x^{(2)}] \in \mathbb{R}^{1 \times d}$, the computation can be expressed:

$$m(x) = m([x^{(1)}, x^{(2)}]) = \max(m(x^{(1)}), m(x^{(2)})), \quad (3)$$

$$f(x) = [e^{m(x^{(1)}) - m(x)} f(x^{(1)}), e^{m(x^{(2)}) - m(x)} f(x^{(2)})], \quad (4)$$

$$\ell(x) = e^{m(x^{(1)}) - m(x)} \ell(x^{(1)}) + e^{m(x^{(2)}) - m(x)} \ell(x^{(2)}), \quad (5)$$

$$\text{softmax}(x) = \frac{f(x)}{\ell(x)}. \quad (6)$$

This decomposition allows for the parallel computation of independent tiles in different PIM devices by maintaining intermediate statistics ($m(x)$, $\ell(x)$). This process, termed **online softmax**, forms the foundation for our PAMattention algorithm.

5.1.2 Token-wise Parallelism. Building on online softmax, the KV cache is partitioned into independent tiles to enable parallel processing [20, 32]. As shown in Figure 5(a), the intermediate outputs are merged through a lightweight reduction step, enabling fine-grained token-wise parallelism. During this procedure, each tile maintains its local maximum and normalization factors (m, l), synchronized during the reduction phase to ensure global consistency.

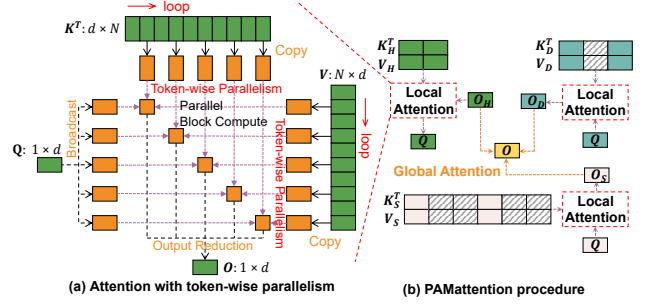


Figure 5: Illustration of PAMattention processing.

5.1.3 Algorithm Design. The key idea of the PAMattention algorithm is to partition the attention workload according to the KV cache locations, distributing them among HBM (K_H, V_H), DDR (K_D, V_D), and SSD (K_S, V_S). The entire procedure, as detailed in Algorithm 1, includes three steps, local attention computation, intra-device and inter-device reduction. First, local attention computation (lines 9-12) is responsible for processing the KV tokens distributed across different locations (e.g., separate banks within the DRAM die). With our token-wise parallelism design, the KV tokens stored at different locations can be processed in parallel. Alongside the two matmul operations ($Q \times K^T$ and $S \times V$), the local function also computes and stores auxiliary scalars m and l for later reduction. Second, intra-device reduction is responsible for merging all outputs in the same PIM device, while inter-device reduction handles all outputs from heterogeneous PIM devices in HBM-PIM. During this reduction procedure (lines 15-22), the global maximum $m^{(t)}$ is first identified. We leverage it to adjust the local output (lines 19-20) and accumulate them in the final result.

Overall, this hierarchical approach minimizes inter-device data transfers, reducing communication overhead while maintaining computational efficiency.

5.2 Architecture Design for PAMattention

As depicted in Figure 6, we propose a multi-tiered design in each PIM device to support PAMattention. The design incorporates local attention Processing Units (PUs) and Reduction Units (RUs) to optimize the computation efficiency of PAMattention.

Algorithm 1: PAMAttention Procedure

Input :KV Cache Matrices $K, V \in \mathbb{R}^{N \times d}$, Vector $Q \in \mathbb{R}^{1 \times d}$;
Output:Vector $O \in \mathbb{R}^{1 \times d}$;

- 1 Divide K, V into three blocks K_H, K_D, K_S and V_H, V_D, V_S according to their storage devices;
- 2 // *Parallel Execution on Heterogeneous PIMs*;
- 3 **Parallel** *for Each block K_i, V_i do*
- 4 $O_i, m_i, \ell_i = \text{Local_Attention}(Q, K_i, V_i);$
- 5 $\vec{O} = [O_H, O_D, O_S], \vec{m} = [m_H, m_D, m_S], \vec{\ell} = [\ell_H, \ell_D, \ell_S];$
- 6 $O, m, \ell = \text{Reduction}(\vec{O}, \vec{m}, \vec{\ell});$
- 7 Return the output $\frac{O}{\ell}$;
- 8
- 9 **Function** Local_Attention(Q, K, V):
- 10 **Parallel** *for $1 \leq j \leq N_i$ do*
- 11 $S^{(j)} = QK_j^T \in \mathbb{R}^{1 \times B_j}; \quad \triangleright K_j \in \mathbb{R}^{B_j \times d};$
- 12 $m^{(j)} = \text{rowmax}(S^{(j)}), \tilde{P}^{(j)} = \exp(S^{(j)} - m^{(j)}),$
- 13 $\ell^{(j)} = \text{rowsum}(\tilde{P}^{(j)}), O^{(j)} = \tilde{P}^{(j)}V_j;$
- 14 $O_i, m_i, \ell_i = \text{Reduction}(\vec{O}, \vec{m}, \vec{\ell});$
- 15 **Function** Reduction($\vec{O}, \vec{m}, \vec{\ell}$):
- 16 *// Find the index t occupies the largest $m^{(t)}$ in \vec{m} ;*
- 17 $m^{(t)} = \max(\vec{m});$
- 18 **for** $O^{(j)}, m^{(j)}, \ell^{(j)} \in \vec{O}, \vec{m}, \vec{\ell}$ **do**
- 19 $\ell^{(j)} = e^{m^{(j)} - m^{(t)}} \cdot \ell^{(j)};$
- 20 $O = O + e^{m^{(j)} - m^{(t)}} \cdot O^{(j)};$
- 21 $\ell = m^{(t)} + \log(\sum(\vec{\ell}));$
- 22 Return $O, m^{(t)}, \ell$

5.2.1 Local Attention Processing Unit (PU). Local Attention Processing Units (PUs) execute the local attention step (line 9) in PAMAttention. As shown in the upper-right corner of Figure 6, each PU includes a specialized Vector Unit for matrix multiplications ($Q \times K^T, S \times V$), built with parallel FP16 multipliers and accumulators. The design is customized per memory tier to balance performance and area constraints:

- PAM-HBM PUs are located near-bank within the DRAM die using a DRAM-compatible process[31, 51, 79]. To match the burst access width of HBM, these PUs feature a 256-bit vector unit (16 FP16 multipliers and adders) and are equipped with a 512-byte local buffer for staging input/output results.
- PAM-DDR PUs also adopt near-bank design and utilize a 64-bit vector unit (4 FP16 multipliers and adders) with a 128-byte buffer.
- PAM-SSD PUs are integrated within the SSD controller. Each controller houses 64 PUs, each equipped with a 256-bit vector unit (16 FP16 multipliers and adders) and a 512-byte buffer.

Each PU also incorporates dedicated circuits for online softmax evaluation. Specifically, a Row-wise Max Unit identifies the maximum value within each assigned row segment, and a lightweight FP16 exponential unit computes element-wise exponentials.

During execution, each PU fetches the query vector Q from its local buffer and directly accesses its assigned KV tokens from the local memory bank, enabling efficient in-place computation of vector products and intermediate statistics in online softmax.

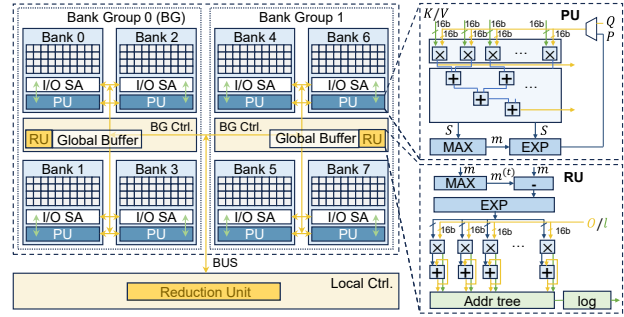


Figure 6: Processing unit designed for PAMAttention.

5.2.2 Reduction Unit (RU). Efficient, scalable reduction is essential for local attention. Without dedicated support, partial outputs must be transferred off-die (e.g., to a logic die), severely underutilizing internal memory bandwidth [106]. To address this, PAM deploys Reduction Units (RUs) in each memory tier to enable in-place, parallel reductions (line 15), maximizing local bandwidth.

Each RU includes a 16-FP16 vector-scalar multiplier, comparator, 4 FP16 exponential units [19], a logarithmic unit, and a 512B scratch buffer for accumulation (Figure 6, bottom-right). A lightweight controller handles input staging and pipelined scheduling for asynchronous execution. The physical placement of RUs varies on different memory devices. a) PAM-HBM: One RU is deployed per bank group, with an additional 128 RUs integrated into the logic die. b) PAM-DDR: One RU is embedded within each DRAM bank group, and 4 additional RUs are placed at the central buffer to aggregate results across chips. c) PAM-SSD: RUs are co-located with the SSD controller. Each controller integrates 8 RUs.

At runtime, RUs fetch partial outputs from their associated PUs or nearby buffers. It determines the row-wise maximum using the comparator, then computes exponentials and accumulates them in its local buffer. Finally, the logarithmic unit performs normalization based on the accumulated sum. This reduction pipeline is fully overlapped with upstream PU execution, supporting continuous streaming of intermediate results without requiring global synchronization. This tiered, distributed RU architecture reduces intra-device transfers by 59%, cuts reduction latency to <2% of PAMAttention time, and improves aggregate reduction bandwidth by 8–12× over centralized schemes [31, 79]. By aligning reduction with memory locality and supporting pipelined execution, PAM sustains high bandwidth across tiers and scales efficiently.

6 PAM: KV-centric Management

The KV-centric management in PAM adopts a token-wise granularity, leveraging token-level parallelism and maximizing context locality benefits. Since KV token placement directly impacts in-memory processing performance, static allocation is suboptimal due to the dynamic nature of activated KV tokens (see §3.3.2). To address these challenges, PAM introduces intra-device KV mapping (§6.1) to fully utilize the internal bandwidth of each PIM device. Furthermore, we propose a novel PAM interface (§6.2) to minimize data transfer overhead across different PIM devices. We also employ a greedy-based KV scheduling strategy (§6.3) to balance computing efficiency across the memory hierarchy.

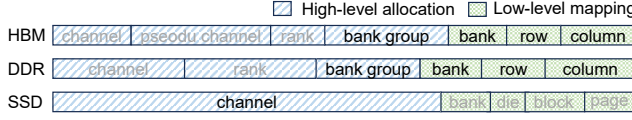


Figure 7: The address illustration of each memory hierarchy.

6.1 Intra-device KV Mapping

Efficient KV token mapping within each device is critical for workload balance and reduced processing latency. PAM leverages token-level parallelism by interleaving KV tokens across bank groups (HBM/DDR) or channels (SSDs). To optimize mapping, PAM adopts a two-level strategy aligned with each memory hierarchy, as shown in Figure 7. The first level assigns KV tokens to bank groups or SSD channels, while the second refines their placement within the selected group or channel.

For high-level allocation, bank groups (or SSD channels) operate in parallel, making the one with the highest processing latency the bottleneck for intra-device mapping (T_{intra}), defined as: $T_{intra} = \max_{bg \in BG} T_{bg}$, where BG represents the set of all bank groups, and T_{bg} denotes the computation latency of a specific bank group. The number of activated KV tokens influences To reduce overall computation latency, PAM balances KV loads across bank groups, as their processing time depends on the number of activated KV tokens, which drive local attention and reduction operations. Based on context locality, PAM first tracks the activation frequency of KV tokens within each bank group over a specified time window (set to 10 decoding processes). Then, KV tokens are greedily allocated to the bank group with the lowest activation frequency, thus balancing the computation load. This strategy is lightweight: for an 80GB HBM stack with 5 devices and 1,280 bank groups [79], only 2.8KB is needed for bank group IDs and under 50KB for activation tracking.

After determining the high-level address, PAM refines internal address mapping based on device-specific access patterns. For HBM and DDR with near-bank designs—where all banks can activate simultaneously [51]—PAM distributes KV tokens evenly across banks to maximize parallel local attention computation. As illustrated in Figure 8(a)(b), banks within a group activate the same rows concurrently, so PAM aligns KV tokens to identical rows and columns across banks, enabling efficient parallelism [79, 116]. Since PAM adopts an on-controller computing design [113] for SSDs, we can easily follow established interleaved storage strategies [43, 53] to boost processing efficiency.

6.2 Inter-device PAM Interface

Efficient intra-PIM computation requires device-specific KV cache layouts, necessitating frequent layout transformations—especially during cross-tier KV transfers. As shown in Figure 8(c), performing these transformations on the host CPU incurs high overhead from CPU-PIM communication and processing latency [72]. This is further exacerbated by PAM’s disabled address hashing, which reduces CPU-side bandwidth to below 10% of optimized levels. Moreover, layout mismatches across devices force costly data exchanges: data must be read into CPU memory, reformatted, and

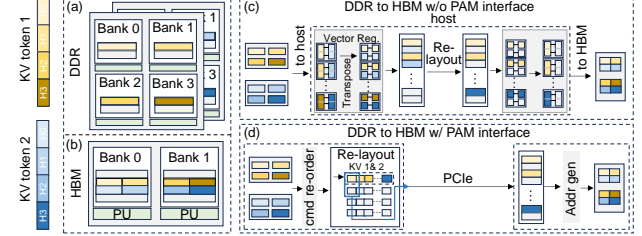


Figure 8: (a)(b) KV token mapping across the banks within bank group; (c) Data layout transformation using host CPU causes frequent CPU-PIM interaction; (d) PAM interface enhances efficient data transfer.

written back—introducing >500ms latency for MB-scale transfers, which is prohibitive for LLM inference.

To this end, PAM introduces a lightweight PAM interface integrated into the memory controller, as shown in Figure 8(d). This interface eliminates repeated CPU involvement by offloading layout transformation and inter-device data movement to hardware. It consists of three key components: (1) a command reorder unit at the sender side, (2) an address generation unit at the receiver side, and (3) a dual-port re-layout buffer shared between them. During data transfer, the command reorder unit organizes memory accesses based on device timing and KV token locations, streaming tokens into the re-layout buffer. Once a contiguous region is assembled, data is transmitted to the target device, where the address generation unit issues parallel write addresses. This hardware-managed path enables format-aware KV token migration. Notably, the combination of re-layout and address generation ensures that data is stored in the expected format for each target device, regardless of the internal data width or address mapping differences. This allows PAM to support heterogeneous memory devices such as HBM and DDR, each with distinct column sizes and address mapping schemes. By removing CPU from the critical path, PAM reduces inter-device transfer latency by more than 20 × and significantly improves scalability by abstracting away layout heterogeneity.

6.3 Inter-device KV Scheduling

Besides achieving load balance in each PIM device, it also requires dynamic migration of KV tokens across memory hierarchy. However, existing data migration strategies, such as FIFO [122, 124] and LRU [1, 26, 128], fail to handle the dynamics, due to their inability to account for the varying contributions of KV tokens. To address this, we introduce a novel importance factor for each KV token, guiding online scheduling and placement across memory tiers to achieve balanced computation.

6.3.1 Evaluating KV Importance. Existing KV sparsity methods [54, 123] provide a performance score $S_i^{(j)}$ to indicate the contribution of each KV token i in the j -th decoding process. However, scores can vary significantly between adjacent steps (e.g., $S_i^{(j-1)}$ and $S_i^{(j)}$) [11]. As a consequence, relying only on the performance score causes massive data migration, which is prohibitively expensive due to the precious inter-device bandwidth. Instead, PAM introduces a novel importance factor $I_i^{(j)}$ as follows.

$$I_i^{(j)} = \lambda S_i^{(j)} + (1 - \lambda) I_i^{(j-1)} \quad (7)$$

In our evaluation, λ is set as 0.6, a hand-crafted value that achieves the best performance in most cases. Instead of using only the current performance score $S_i^{(j)}$, PAM also considers the temporal importance factor $I_i^{(j-1)}$ of the previous step to estimate the significance of each KV token. This enables slight adjustments on the importance factors during decoding. Then, we further evaluate the importance of all KV tokens stored on a particular device:

$$IS_{\mathbb{D}}^{(j)} = \frac{\sum_{i \in \mathbb{D}} I_i^{(j)}}{\#KV \text{ tokens}} \quad (8)$$

where $IS_{\mathbb{D}}^{(j)}$ is the cumulative importance score of all KV tokens ($\#KV \text{ tokens}$) stored on device \mathbb{D} at step j . This enables more informed load-balancing decisions across heterogeneous PIM devices.

6.3.2 Greedy Scheduling Algorithm. The KV scheduling strategy aims to balance the computation load across heterogeneous devices by adjusting the stored locations of KV tokens, based on our predefined importance ratios of balance:

$$IS_H^{(j)} : IS_{\mathbb{D}}^{(j)} : IS_S^{(j)} = x : y : 1 \quad (9)$$

where IS_H , $IS_{\mathbb{D}}$ and IS_S indicate the importance score of HBM, DDR and SSD, respectively. The predefined ratios x and y , obtained via offline profiling, remain fixed during execution. We explore various x, y configurations across datasets to identify the optimal settings for cross-device load balancing. Our results show that parameters x and y are architecture-dependent but workload-agnostic, thanks to the attention sparsity algorithm [86, 123]. This approach normalizes token scores across datasets, eliminating the need for workload-specific tuning. Thus, x and y only require adjustment when deploying new LLM architectures.

Bearing the goals of fast and minimal-data-movement load-balancing, we propose a simple yet effective greedy online scheduling strategy. As shown in Algorithm 2, we adjust the locations of KV tokens based on the predefined ratios with two steps.

Algorithm 2: Online KV Scheduling

Input :Importance Score $IS_H^{(j)}, IS_{\mathbb{D}}^{(j)}, IS_S^{(j)}$;
 Predetermined Ratio x, y ;
Output:Updated KV Management Table;

```

1  $x^* = \frac{IS_H^{(j)}}{IS_S^{(j)}}, y^* = \frac{IS_{\mathbb{D}}^{(j)}}{IS_S^{(j)}}$ ;  $\triangleright$  Compute the corresponding ratio;
2 while  $(x^* + y^*) < (x + y)$  do
3   Find the least importance KV token in DDR  $\mathbb{D}_r$ ;
4   Find the most important KV token in SSD  $\mathbb{S}_t$ ;
5   Swap the corresponding KV token  $\mathbb{D}_r \leftrightarrow \mathbb{S}_t$ ;
6   Update  $x^*, y^*$ ;
7 while  $\frac{x^*}{y^*} < \frac{x}{y}$  do
8   Find the least importance KV token in HBM  $\mathbb{H}_r$ ;
9   Find the most important KV token in DDR  $\mathbb{D}_t$ ;
10  Swap the corresponding KV token  $\mathbb{H}_r \leftrightarrow \mathbb{D}_t$ ;
11  Update  $x^*, y^*$ ;

```

We initially treat HBM and DDR as a unified device and check if the current KV token distribution matches the target ratio. If low-importance tokens exceed the threshold in DDR, we swap the least important DDR tokens with the most important ones in SSD (lines 3–6). After balancing SSD, the strategy manages KV cache between HBM and DDR similarly (lines 8–11), adjusting only when higher-bandwidth devices hold lower-importance tokens, since low-cost memory is bandwidth-limited. This greedy approach reduces token movement overhead while enabling real-time scheduling. Specifically, our evaluation demonstrates that only 0.7% of the total KV tokens require adjustment, with SSD-to-DDR data transfers accounting for less than 0.1% in each decoding step. However, since important-token divergence accumulates over steps (see Figure 3), it is still necessary to adjust inter-device KV placement (evaluation in §7.4). Consequently, the lightweight scheduler minimizes unnecessary data movement and ensures a load-balanced processing across PIM tiers, at negligible runtime cost.

7 Evaluation

7.1 Evaluation Methodology

Baseline Systems. We compare PAM against four systems (vLLM-offloading, AttAcc!, L-PIM and LS-PIM) on a heterogeneous platform (8×H100-80GB GPUs, 1280GB DDR4, 8TB SSD), comparable to DGX-H100 [75] and EC2 p5.48xlarge [7].

vLLM-offloading (GPU-only): vLLM [46] is a high-throughput serving engine managed with paged attention [45], optimized with FlashAttention and FlashDecoding [21, 109]. We extend it with a hierarchical memory design, adopting DeepSpeed-Inference [8]’s offloading to satisfy the memory demands of large-scaling serving.

AttAcc! (GPU+HBM-PIM): AttAcc! [79] integrates HBM-PIM to boost GPU cluster performance by offloading attention while assigning FC operations to GPUs. It does not support KV cache offloading to host memory or SSD.

L-PIM & LS-PIM (GPU+Layered PIM): To assess PAM’s benefits, we include L-PIM and LS-PIM, which use layered PIM in multi-GPU setups. L-PIM mimics AttAcc!, prioritizing KV cache in higher memory tiers. LS-PIM further utilizes KV sparsity to reduce compute and loading overhead. Neither adopts our PAMattention mechanism or KV management strategies.

Simulation. We built an in-house simulator to evaluate PAM and baseline systems, avoiding cross-platform discrepancies consistently. It integrates multiple open-source tools, including LLM-ServingSim [16], LLMCompass [130], Ramulator 2.0 [63, 88], and OpenSSD [105], with several key enhancements: 1) GPU Simulation: LLMCompass models operators’ performance that run on GPUs. 2) KV Transfer & Computation: Ramulator and OpenSSD are extended to simulate KV token transfers and PIM processing across the memory hierarchy. 3) Interaction and System Scheduling: LLM-ServingSim is modified to simulate data interaction between GPUs and tiered-PIMs, as well as achieving memory management and online scheduling for PAM system. The evaluation results are cross-verified with the vLLM-based system and AttAcc! simulator. These changes enable accurate performance simulation across diverse hardware configurations. We use 4-way tensor and 2-way pipeline parallelism as a representative setup.

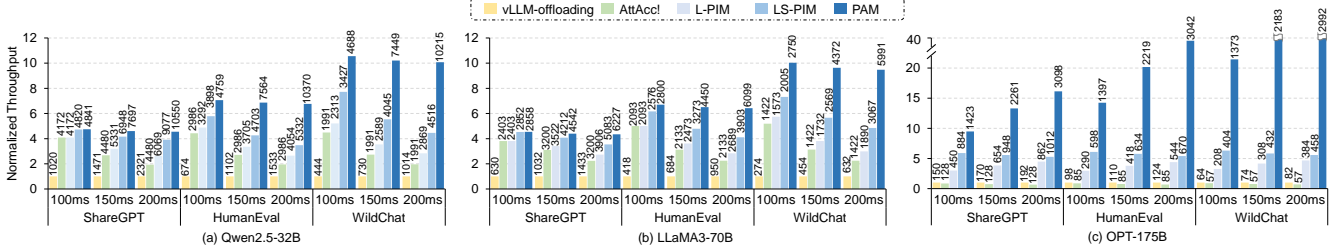


Figure 9: The normalized throughput of various SLOs for (a) Qwen2.5-32B (b) LLaMA3-70B (c) OPT-175B. Each number above the bar indicates the maximum batch size per system considering the SLO and capacity limitations.

Table 1: Configuration details of PAM.

HBM Parameters	
HBM3 5.2Gbps, 16GB/HBMx40, 16 channel/HBM	
2 pseudo channel/ch, 2 rank/pch, 4 bank groups/rank, 4 bank/BG	
HBM Timing	
tRP=19, tRCD=19, tRAS=45, tRDL=4	
tCCD_S=2, tCCD_L=4, tWR=21, tREFI=5070, tFAW=39	
DDR Parameters	
DDR4-3200, 32GB/DDR×40, 2 rank/DDR, 8 chip/rank, 2 bank groups/chip, 4 bank/BG	
DDR Timing	
tRC=76, tRCD=24, tCL=24, tRP=24, tBL=4	
tCCD_S=4, tCCD_L=8, tRRD_S=4, tRRD_L=6, tFAW=26	
SSD Parameters & Timing	
256GB/channel × 64, 4 die per channel, page size = 16KB, 2400MT/s, tR = 30us	

Hardware Specifications. Table 1 outlines the PAM’s configuration. Each HBM/DDR4 channel contains 64/128 PIM banks, while each SSD has 8 channels. The operating frequencies of PUs are set to 666MHz (HBM), 500MHz (DDR), and 1GHz (SSD). Power estimates are derived from Ramulator 2.0 and OpenSSD, using voltage and current values from publicly available specifications for HBM3 [79, 80], DDR4 [9, 23], and SSD controllers [67]. Following prior work [52, 92], PU power is assumed to be 3× that of a standard read. Under peak power constraints [9, 50, 79], the per-device compute capacity is 1.6 TFLOPS (HBM), 204 GFLOPS (DDR), and 18 GFLOPS (SSD). These settings are configurable—PAM’s architecture is orthogonal to specific configurations, enabling flexibility.

Evaluation workloads. To capture real-world LLM serving scenarios, we evaluate PAM on two workload types: online dialogue tasks and offline long-text processing tasks.

For *online dialogue tasks*, we utilize three real-world datasets: 1) ShareGPT [101] includes a set of conversations scraped from real-world user logs of ChatGPT [77]. 2) WildChat [134] has a corpus of 1 million real-world user-ChatGPT interactions. 3) HumanEval [12] contains 164 programming problems with a function signature or docstring to evaluate code completion performance. These online dialogue tasks usually take a few hundred tokens to complete (the average input/output sequence length is 183/299).

For *offline tasks*, we evaluate document summarization using the following datasets: 1) Arxiv_sum [17] is a dataset to estimate the summarization capability for academic papers from arXiv. 2) Write_doc [49] is a benchmark designed to evaluate the performance of writing documents. These offline tasks typically involve long-context processing with a sequence length ranging from 1500 ~ 8000, requiring substantial memory capacity.

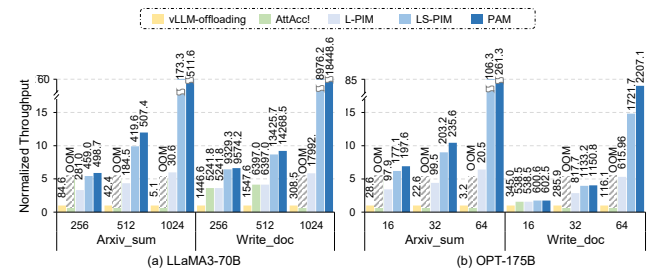


Figure 10: The normalized throughput of various batch sizes for offline tasks. Each number above the bar indicates the throughput under the batch size. OOM means out of memory.

LLMs & Algorithms. We test PAM using three open-source LLMs: Qwen2.5-32B [100], LLaMA3-70B [24], and OPT-175B [131]. In our experiments, all models employ 16-bit floating-point precision (BF16/FP16) for computation, with both weights and KV cache stored in 16-bit floating-point format. Furthermore, all models leverage the state-of-the-art KV sparsity algorithm [123] with 8× compression. The compression yields negligible accuracy loss (under 1%) across all workloads. Importantly, PAM’s KV management is algorithm-agnostic, supporting diverse compression methods.

Evaluation Metrics. For *online serving*, we measure peak throughput under Service Level Objective (SLO) constraints to ensure real-time responsiveness. For *offline tasks*, we report maximum throughput at a fixed batch size, capturing the system’s efficiency in handling large batches and long-context processing.

7.2 PAM Performance

Online Serving under diverse SLOs. For online tasks, we set SLOs at 100 ms, 150 ms, and 200 ms—faster than typical human reading speeds [104]. As shown in Figure 9, PAM consistently supports the largest batch sizes across diverse SLOs. Compared to vLLM-offloading, PAM delivers average throughput gains of 7.20× (Qwen2.5-32B), 6.93× (LLaMA3-70B), and 24.53× (OPT-175B).

PAM shows lower normalized throughput gains on Qwen2.5-32B and LLaMA3-70B than on OPT-175B, as smaller models impose less KV cache pressure. Under the given SLO of 100 ms for ShareGPT, vLLM-offloading keeps the KV cache within HBM for both Qwen2.5-32B and LLaMA3-70B, avoiding performance drops. In this case, AttAcc! achieves the same serving performance as L-PIM. In contrast, serving OPT-175B always exceeds HBM capacity, sharply

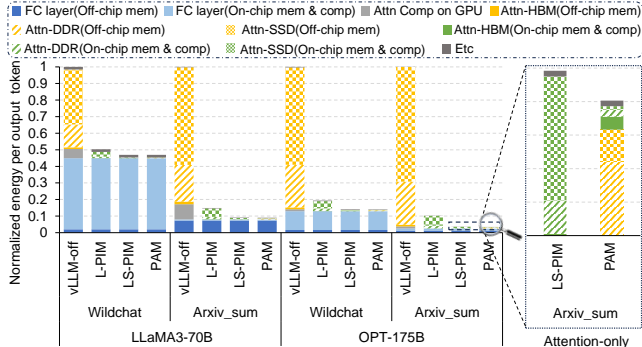


Figure 11: The normalized energy per output token for LLaMA3-70B and OPT-175B.

reducing the supported batch size of vLLM-offloading. L-PIM and LS-PIM encounter similar limitations. Fortunately, PAM overcomes this by efficiently leveraging context locality, maintaining strong performance even when KV cache exceeds both HBM and DDR capacity. In particular, PAM achieves an average 4.54 \times throughput gain over LS-PIM in various cases.

PAM’s performance gains vary across datasets. It achieves an average improvement of 13.76 \times on WildChat versus 6.12 \times on ShareGPT compared to vLLM-offloading. This discrepancy stems from WildChat’s longer average context (738 tokens on average vs. 534 in ShareGPT), which increases the proportion of attention computation—the part PAM optimizes effectively. Longer contexts also require more KV cache capacity, which PAM handles efficiently through its hierarchical memory design and KV management.

Offline End-to-End Throughput. We evaluate PAM on offline tasks using LLaMA3-70B (batch sizes: 256, 512, 1024) and OPT-175B (batch sizes: 16, 32, 64), as shown in Figure 10. PAM consistently achieves the highest throughput, with performance gains increasing at larger batch sizes.

For LLaMA3-70B, PAM improves throughput by 39.2 \times (Arxiv_sum) and 25.2 \times (write_doc) over vLLM-offloading. For OPT-175B, gains reach 33.0 \times and 8.26 \times , respectively. These improvements arise as large batches increase KV demands, often exceeding HBM/DDR capacity. AttAcc! fails in most cases due to lack of KV offloading support, while vLLM-offloading, L-PIM, and LS-PIM are bottlenecked by DDR/SSD bandwidth. For example, in L-PIM, SSD holds >65% of KV data but consumes >93% of compute time. LS-PIM relies on static KV placement, underutilizing HBM. In contrast, PAM sustains high throughput by combining PAMAttention with dynamic KV scheduling, effectively leveraging context locality and balancing load across memory tiers for long-context workloads.

In summary, PAM is particularly well-suited for scenarios involving large-scale LLMs, large batch sizes, and long context lengths. Given the widely adopted scaling law [41] and chain-of-thought [112, 125], which requires larger-scale LLMs and longer context, PAM provides promising superiority for future LLM serving.

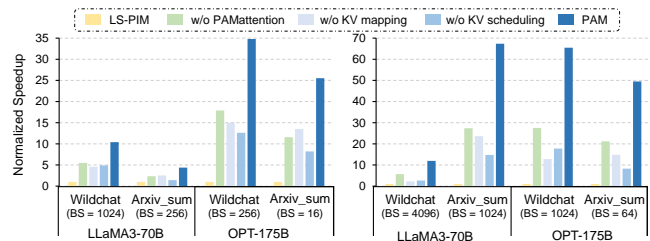


Figure 12: Ablation study on proposed PAMAttention and KV-centric management strategies.

7.3 Energy Efficiency

We evaluate PAM’s energy breakdown using LLaMA3-70B and OPT-175B on Wildchat and Arxiv_sum. For online tasks, batch sizes are 8192 (LLaMA3) and 512 (OPT); for offline, 1024 and 64, respectively.

As shown in Figure 11, PAM reduces power by 53.1%~92.7% vs. vLLM-offloading, 7.8%~66.9% vs. L-PIM, and 4.0%~18.7% (attention only) vs. LS-PIM. Gains over vLLM-offloading come from avoiding excessive off-chip KV transfers—e.g., OPT-175B on Arxiv_sum incurs 2304 GB of KV movement (>95% energy) in vLLM-offloading, which PAM largely eliminates. Compared to L-PIM, PAM’s sparse attention reduces both compute and memory energy. LS-PIM’s savings are outpaced by PAM’s improved locality and scheduling, which shift more work to energy-efficient HBM. Although PAM incurs inter-device transfers, its tiered RU design and KV scheduling keep overall energy lower, as shown in Figure 11.

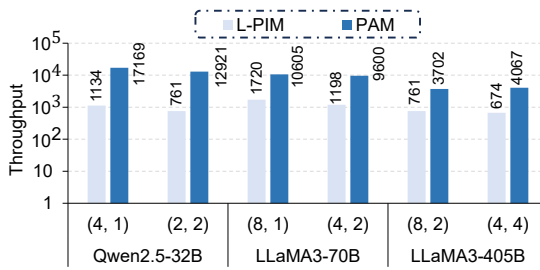
7.4 Ablation Study

To evaluate the techniques in §5 and §6, we compare normalized attention computation speedups across LLMs and optimization strategies, using LS-PIM as the baseline (normalized to 1). “w/o PAMAttention” uses fixed tiling as in FlashAttention and FlashDecoding [21, 109]; “w/o KV mapping” balances device loads but applies naive KV distribution, ignoring access frequency; and “w/o KV scheduling” disables inter-device scheduling, keeping KV in its original placement. Figure 12 shows results under two batch sizes.

In the small batch setting (left of Figure 12), PAM achieves a 18.7 \times average speedup over LS-PIM, and 1.93 \times , 2.06 \times , and 2.74 \times over the “w/o PAMAttention,” “w/o KV mapping,” and “w/o scheduling” variants, respectively. In large batches (right), PAM’s gains rise to 48.56 \times over LS-PIM, and 2.35 \times , 4.15 \times , and 4.62 \times over the baselines. These improvements stem from PAM’s ability to exploit context locality and mitigate bottlenecks in low-bandwidth devices (e.g., SSDs), where LS-PIM suffers from KV overload. Without KV scheduling, cross-tier load balancing remains ineffective. Specifically, while only a small number of KV tokens migrate per decoding step, significant divergence in important KV tokens accumulates over multiple steps. Consequently, the absence of KV scheduling severely impacts attention computation performance, particularly in long-context generation scenarios. PAM overcomes this via intra-device mapping and inter-device scheduling. Additionally, PAMAttention consistently improves performance across models due to shared LLM attention structures, with larger KV caches amplifying the benefits of mapping and scheduling.

Table 2: The additional area of PAM in the memory hierarchy.

Components		Area (mm ²)	Area Ratio
HBM-PIM	PU & RU	11.2mm ²	9.25% (of dram die [80])
	PAM interface	0.85mm ²	0.703% (of logic die)
DDR-PIM	PU & RU	5.04mm ²	5.04% (of dram chip [91])
	PAM interface	0.85mm ²	0.750% (of center buffer)
SSD-PIM	PU & RU	8.16mm ²	7.592% (of Controller [103])
	PAM interface	0.85mm ²	0.578% (of Controller)

**Figure 13: Throughput of scaled PAM systems with different numbers of PAM instances under tensor parallelism (TP) and pipeline parallelism (PP), noted as (TP, PP).**

7.5 Area Cost Evaluation

The area overhead of PAM mainly arises from integrating Processing Units (PUs), Reduction Units (RUs), and PAM interface logic. We implemented these modules in Verilog and synthesized them using Synopsys Design Compiler [98]. For HBM-PIM and DDR-PIM, PUs and RUs are synthesized in DRAM-compatible 1z-nm and 2x-nm processes [9, 23, 80], which are 10 \times less dense than logic processes[23]. The PAM interface and SSD-side logic (PUs, RUs) are synthesized in TSMC 14nm [67, 103].

For the HBM-PIM configuration, the additional logic occupies 11.2mm² per DRAM die, 9.25% of a typical 121mm² HBM3 die [80]. Each DRAM die integrates 64 PUs (0.13mm² each) and 16 RUs (0.18mm² each). Within each PU, the area is distributed among compute datapaths (67%), buffer storage (11%), and control logic (22%). In the RU, approximately 83% of the area is dedicated to computing logic.² For the DDR-PIM configuration, each DRAM chip integrates 8 PUs and 2 RUs, contributing a total area overhead of 5.04mm², or 5.04% of a typical 100mm² DDR4 die [23]. The area of each PU and RU is 0.46mm² and 0.68mm², respectively. In the SSD-PIM, the compute extensions—including 64 PUs, 8 RUs, and a shared buffer—occupy an additional 8.16mm², accounting for 7.59% of a typical SSD controller area [103]. Overall, the added logic is modest and remains within feasible die area budgets under current manufacturing constraints. The overhead is well-justified by the substantial performance gains reported in our evaluation.

7.6 Scalability

To evaluate PAM’s scalability, we ran experiments using the Write_doc task with 1024 requests, scaling the number of GPUs and storage devices proportionally. The system was extended using standard tensor parallelism (TP) and pipeline parallelism (PP). As shown in Figure 13, PAM consistently outperforms L-PIM, achieving 6.03 \times –16.96 \times higher performance across configurations, demonstrating strong scalability. TP generally yields higher throughput than PP, as PP suffers from pipeline bubbles and added latency. However, TP’s communication overhead grows with scale, becoming a key consideration for large deployments.

8 Conclusion

We present PAM, an innovative LLM serving system that optimizes costly KV-related operations. PAM integrates processing units within memory devices and introduces a "processing across memory" paradigm to address the high memory bandwidth and capacity demands of LLM serving. Leveraging intrinsic context locality, PAM enables efficient KV allocation across the memory hierarchy. We also propose PAMAttention, a novel algorithm using token-wise parallelism to support attention computation across heterogeneous PIM devices. Additionally, PAM implements high-performance KV management through intra-device KV mapping and inter-device KV scheduling, balancing attention computations across the memory hierarchy. Overall, PAM enhances LLM serving efficiency, enabling cost-effective large-scale AI deployment.

References

- [1] [n. d.]. Memcached. <https://memcached.org/>.
- [2] Josh Achiam, Steven Adler, Sandhini Agarwal, Lama Ahmad, Ilge Akkaya, Florencia Leoni Aleman, Diogo Almeida, Janko Altenschmidt, Sam Altman, Shyamal Anadkat, et al. 2023. Gpt-4 technical report. *arXiv preprint arXiv:2303.08774* (2023).
- [3] Amey Agrawal, Nitin Kedia, Ashish Panwar, Jayashree Mohan, Nipun Kwatra, Bhargav Gulavani, Alexey Tumanov, and Ramachandran Ramjee. 2024. Taming {Throughput-Latency} Tradeoff in {LLM} Inference with {Sarahi-Serve}. In *18th USENIX Symposium on Operating Systems Design and Implementation (OSDI 24)*. 117–134.
- [4] Keivan Alizadeh, Iman Mirzadeh, Dmitry Belenko, Karen Khatamifard, Minsik Cho, Carlo C Del Mundo, Mohammad Rastegari, and Mehrdad Farajtabar. 2023. Llm in a flash: Efficient large language model inference with limited memory. *arXiv preprint arXiv:2312.11514* (2023).
- [5] James Allen. 1988. *Natural language understanding*. Benjamin-Cummings Publishing Co., Inc.
- [6] Bowen Alpern, Larry Carter, Ephraim Feig, and Ted Selker. 1994. The uniform memory hierarchy model of computation. *Algorithmica* 12 (1994), 72–109.
- [7] Amazon AWS Group. 2024. Amazon EC2 p5.48xlarge Instance. <https://aws.amazon.com/ec2/instance-types/p5>.
- [8] Reza Yazdani Aminabadi, Samyam Rajbhandari, Ammar Ahmad Awan, Cheng Li, Du Li, Elton Zheng, Olatunji Ruwase, Shaden Smith, Minjia Zhang, Jeff Rasley, et al. 2022. Deepspeed-inference: enabling efficient inference of transformer models at unprecedented scale. In *SC22: International Conference for High Performance Computing, Networking, Storage and Analysis*. IEEE, 1–15.
- [9] JEDEC Solid State Technology Association. 2012. *DDR4 SDRAM Standard*. Standard JESD79-4. JEDEC Solid State Technology Association.
- [10] Xuyi Cai, Ying Wang, and Lei Zhang. 2022. Optimus: An operator fusion framework for deep neural networks. *ACM Transactions on Embedded Computing Systems* 22, 1 (2022), 1–26.
- [11] Zefan Cai, Yichi Zhang, Bofei Gao, Yuliang Liu, Tianyu Liu, Keming Lu, Wayne Xiong, Yue Dong, Baobao Chang, Junjie Hu, et al. 2024. Pyramidkv: Dynamic kv

²Compared to general-purpose designs such as Samsung’s HBM-PIM[51] and UPMEM[23], the additional logic in our design omits complex control units, which contributes to a notable reduction in area cost. Furthermore, for the HBM-PIM case, our evaluation assumes an HBM3-based implementation using a more advanced process node. If synthesized using the same older technology node as Samsung’s HBM-PIM, the total area overhead would increase to 23.4mm² out of 84.4mm² (~ 27.7%).

cache compression based on pyramidal information funneling. *arXiv preprint arXiv:2406.02069* (2024).

[12] Mark Chen, Jerry Tworek, Heewoo Jun, Qiming Yuan, Henrique Ponde De Oliveira Pinto, Jared Kaplan, Harri Edwards, Yuri Burda, Nicholas Joseph, Greg Brockman, et al. 2021. Evaluating large language models trained on code. *arXiv preprint arXiv:2107.03374* (2021).

[13] Shaoyuan Chen, Yutong Lin, Mingxing Zhang, and Yongwei Wu. 2024. Efficient and Economic Large Language Model Inference with Attention Offloading. *arXiv preprint arXiv:2405.01814* (2024).

[14] Wei-Lin Chiang, Zhuohan Li, Zi Lin, Ying Sheng, Zhanghao Wu, Hao Zhang, Lianmin Zheng, Siyuan Zhuang, Yonghao Zhuang, Joseph E Gonzalez, et al. 2023. Vicuna: An open-source chatbot impressing gpt-4 with 90%* chatgpt quality. *See https://vicuna.lmsys.org (accessed 14 April 2023)* 2, 3 (2023), 6.

[15] Wei-Lin Chiang, Lianmin Zheng, Ying Sheng, Anastasios Nikolaos Angelopoulos, Tianle Li, Dacheng Li, Hao Zhang, Banghua Zhu, Michael Jordan, Joseph E Gonzalez, et al. 2024. Chatbot arena: An open platform for evaluating llms by human preference. *arXiv preprint arXiv:2403.04132* (2024).

[16] Jaehong Cho, Minsu Kim, Hyunmin Choi, Guseul Heo, and Jongse Park. 2024. LLMervingSim: A HW/SW Co-Simulation Infrastructure for LLM Inference Serving at Scale. *arXiv preprint arXiv:2408.05499* (2024).

[17] Arman Cohan, Francis Dernoncourt, Doo Soon Kim, Trung Bui, Seokhwan Kim, Walter Chang, and Nazli Goharian. 2018. A Discourse-Aware Attention Model for Abstractive Summarization of Long Documents. In *Proceedings of the 2018 Conference of the North American Chapter of the Association for Computational Linguistics: Human Language Technologies, Volume 2 (Short Papers)*. Association for Computational Linguistics, New Orleans, Louisiana, 615–621. <https://doi.org/10.18653/v1/N18-2097>

[18] Edward I. Cohen, Gary M. King, and James T. Brady. 1989. Storage hierarchies. *IBM Systems Journal* 28, 1 (1989), 62–76.

[19] Patrícia da Costa, Morgana da Rosa, Guilherme Paim, Eduardo da Costa, Rafael Soares, and Sergio Bampi. 2022. An efficient exponential unit designed in VLSI CMOS with custom operators. In *2022 29th IEEE International Conference on Electronics, Circuits and Systems (ICECS)*. IEEE, 1–4.

[20] Tri Dao. 2024. FlashAttention-2: Faster Attention with Better Parallelism and Work Partitioning. In *The Twelfth International Conference on Learning Representations*.

[21] Tri Dao, Dan Fu, Stefano Ermon, Atri Rudra, and Christopher Ré. 2022. Flashattention: Fast and memory-efficient exact attention with io-awareness. *Advances in Neural Information Processing Systems* 35 (2022), 16344–16359.

[22] Yichuan Deng, Zhao Song, and Chiwun Yang. 2024. Attention is Naturally Sparse with Gaussian Distributed Input. *arXiv preprint arXiv:2404.02690* (2024).

[23] Fabrice Devaux. 2019. The true processing in memory accelerator. In *2019 IEEE Hot Chips 31 Symposium (HCS)*. IEEE Computer Society, 1–24.

[24] Abhimanyu Dubey, Abhinav Jauhri, Abhinav Pandey, Abhishek Kadian, Ahmad Al-Dahle, Aiesha Letman, Akhil Mathur, Alan Schelten, Amy Yang, Angela Fan, et al. 2024. The llama 3 herd of models. *arXiv preprint arXiv:2407.21783* (2024).

[25] Daichi Fujiki, Alireza Khadem, Scott Mahlke, and Reetuparna Das. 2022. Multi-Layer In-Memory Processing. In *2022 55th IEEE/ACM International Symposium on Microarchitecture (MICRO)*. IEEE, 920–936.

[26] Bin Gao, Zhuomin He, Puru Sharma, Qinxuan Kang, Djordje Jevdjic, Junbo Deng, Xingkun Yang, Zhou Yu, and Pengfei Zuo. 2024. {Cost-Efficient} Large Language Model Serving for Multi-turn Conversations with {CachedAttention}. In *2024 USENIX Annual Technical Conference (USENIX ATC 24)*, 111–126.

[27] Juan Gómez-Luna, Izzat El Hajj, Ivan Fernandez, Christina Giannoula, Geraldo F Oliveira, and Onur Mutlu. 2021. Benchmarking memory-centric computing systems: Analysis of real processing-in-memory hardware. In *2021 12th International Green and Sustainable Computing Conference (IGSC)*. IEEE, 1–7.

[28] Daya Guo, Dejian Yang, Haowei Zhang, Junxiao Song, Ruoyu Zhang, Runxin Xu, Qihao Zhu, Shirong Ma, Peiyi Wang, Xiao Bi, et al. 2025. Deepseek-r1: Incentivizing reasoning capability in llms via reinforcement learning. <https://chat.deepseek.com>

[29] Jiao He and Jidong Zhai. 2024. FastDecode: High-Throughput GPU-Efficient LLM Serving using Heterogeneous Pipelines. *arXiv preprint arXiv:2403.11421* (2024).

[30] Mingxuan He, Choungki Song, Ilkon Kim, Chunseok Jeong, Seho Kim, Il Park, Mithuna Thottethodi, and TN Vijaykumar. 2020. Newton: A DRAM-maker’s accelerator-in-memory (AiM) architecture for machine learning. In *2020 53rd Annual IEEE/ACM International Symposium on Microarchitecture (MICRO)*. IEEE, 372–385.

[31] Guseul Heo, Sangyeop Lee, Jaehong Cho, Hyunmin Choi, Sanghyeon Lee, Hyungkyu Ham, Gwangsun Kim, Divya Mahajan, and Jongse Park. 2024. Ne-upims: Npu-pim heterogeneous acceleration for batched llm inferencing. In *Proceedings of the 29th ACM International Conference on Architectural Support for Programming Languages and Operating Systems, Volume 3*. 722–737.

[32] Ke Hong, Guohao Dai, Jiaming Xu, Qiuli Mao, Xiuhong Li, Jun Liu, Yuhang Dong, Yu Wang, et al. 2024. FlashDecoding++: Faster Large Language Model Inference with Asynchronization, Flat GEMM Optimization, and Heuristics. *Proceedings of Machine Learning and Systems* 6 (2024), 148–161.

[33] Ranggi Hwang, Jianyu Wei, Shijie Cao, Changho Hwang, Xiaohu Tang, Ting Cao, and Mao Yang. 2024. Pre-gated moe: An algorithm-system co-design for fast and scalable mixture-of-expert inference. In *2024 ACM/IEEE 51st Annual International Symposium on Computer Architecture (ISCA)*. IEEE, 1018–1031.

[34] Shashank Mohan Jain. 2022. Hugging face. In *Introduction to transformers for NLP: With the hugging face library and models to solve problems*. Springer, 51–67.

[35] Hongsun Jang, Jaeyong Song, Jaewon Jung, Jaeyoung Park, Youngsok Kim, and Jinho Lee. 2024. Smart-Infinity: Fast Large Language Model Training using Near-Storage Processing on a Real System. In *2024 IEEE International Symposium on High-Performance Computer Architecture (HPCA)*. IEEE, 345–360.

[36] Huiqiang Jiang, YUCHENG LI, Chengruidong Zhang, Qianhui Wu, Xufang Luo, Surin Ahn, Zhenhua Han, Amit H Abdi, Dongsheng Li, Chin-Yew Lin, et al. [n.d.]. MInference 1.0: Accelerating Pre-filling for Long-Context LLMs via Dynamic Sparse Attention. In *The Thirty-eighth Annual Conference on Neural Information Processing Systems*.

[37] Xuanlin Jiang, Yang Zhou, Shiyi Cao, Ion Stoica, and Minlan Yu. 2024. NEO: Saving GPU Memory Crisis with CPU Offloading for Online LLM Inference. *arXiv preprint arXiv:2411.01142* (2024).

[38] Norm Jouppi, George Kurian, Sheng Li, Peter Ma, Rahul Nagarajan, Lifeng Nai, Nishant Patil, Suvinay Subramanian, Andy Swing, Brian Towles, et al. 2023. Tpu v4: An optically reconfigurable supercomputer for machine learning with hardware support for embeddings. In *Proceedings of the 50th Annual International Symposium on Computer Architecture*. 1–14.

[39] Norman P Jouppi, Cliff Young, Nishant Patil, David Patterson, Gaurav Agrawal, Raminder Bajwa, Sarah Bates, Suresh Bhatia, Nan Boden, Al Borchers, et al. 2017. In-datacenter performance analysis of a tensor processing unit. In *Proceedings of the 44th annual international symposium on computer architecture*. 1–12.

[40] Abdullah Talha Kabakuş and İbrahim Dogru. 2024. The battle of Chatbot Giants: an experimental comparison of ChatGPT and Bard. *International Journal of Engineering Research and Development* 16, 2 (2024), 679–691.

[41] Jared Kaplan, Sam McCandlish, Tom Henighan, Tom B Brown, Benjamin Chess, Rewon Child, Scott Gray, Alec Radford, Jeffrey Wu, and Dario Amodei. 2020. Scaling laws for neural language models. *arXiv preprint arXiv:2001.08361* (2020).

[42] Jinkyum Kim, Myeonggu Kang, Yunki Han, Yang-Gon Kim, and Lee-Sup Kim. 2023. Optimstore: In-storage optimization of large scale dnns with on-die processing. In *2023 IEEE International Symposium on High-Performance Computer Architecture (HPCA)*. IEEE, 611–623.

[43] Jesung Kim, Jong Min Kim, Sam H Noh, Sang Lyul Min, and Yookun Cho. 2002. A space-efficient flash translation layer for compactflash systems. *IEEE Transactions on Consumer Electronics* 48, 2 (2002), 366–375.

[44] Jin Hyun Kim, Yuhwan Ro, Jinin So, Sukhan Lee, Shin-haeng Kang, YeonGon Cho, Hyeonsu Kim, Byeongho Kim, Kyungsoo Kim, Sangsoo Park, et al. 2023. Samsung pim/pnm for transpiler based ai: Energy efficiency on pim/pnm cluster. In *2023 IEEE Hot Chips 35 Symposium (HCS)*. IEEE Computer Society, 1–31.

[45] Woosuk Kwon, Zhuohan Li, Siyuan Zhuang, Ying Sheng, Lianmin Zheng, Cody Hao Yu, Joseph Gonzalez, Hao Zhang, and Ion Stoica. 2023. Efficient memory management for large language model serving with paggedattention. In *Proceedings of the 29th Symposium on Operating Systems Principles*. 611–626.

[46] Woosuk Kwon, Zhuohan Li, Siyuan Zhuang, Ying Sheng, Lianmin Zheng, Cody Hao Yu, Joseph E. Gonzalez, Hao Zhang, and Ion Stoica. 2023. vLLM: Easy, fast, and cheap LLM serving for everyone. <https://github.com/vllm-project/vllm>

[47] Yongkee Kwon, Kornijcuk Vladimir, Nahsung Kim, Woojae Shin, Jongsoon Won, Minkyu Lee, Hyunwoo Joo, Haerang Choi, Guhyun Kim, Byeongju An, et al. 2022. System architecture and software stack for GDDR6-AiM. In *2022 IEEE Hot Chips 34 Symposium (HCS)*. IEEE, 1–25.

[48] M. Lammertyn. 2024. 60+ ChatGPT Statistics And Facts You Need to Know. <https://blog.ingvate.com/chatgpt-statistics>

[49] Lance Xiao. 2024. Datasets to doc writing. https://huggingface.co/datasets/lancexiao/write_doc_sft_v1

[50] Joo Hwan Lee, Hui Zhang, Veronica Lagrange, Praveen Krishnamoorthy, Xiaodong Zhao, and Yang Seok Ki. 2020. SmartSSD: FPGA accelerated near-storage data analytics on SSD. *IEEE Computer architecture letters* 19, 2 (2020), 110–113.

[51] Sukhan Lee, Shin-haeng Kang, Jaehoon Lee, Hyeonsu Kim, Eojin Lee, Seungwoo Seo, Hosang Yoon, Seungwon Lee, Kyounghwan Lim, Hyunsung Shin, et al. 2021. Hardware architecture and software stack for PIM based on commercial DRAM technology: Industrial product. In *2021 ACM/IEEE 48th Annual International Symposium on Computer Architecture (ISCA)*. IEEE, 43–56.

[52] Seongju Lee, Kyuyoung Kim, Sanghoon Oh, Joonhong Park, Gimoong Hong, Dongyoon Ka, Kyudong Hwang, Jeongja Park, Kyeongpil Kang, Jungyeon Kim, et al. 2022. A 1ynm 1.25 V 8Gb, 16Gb/s/pin GDDR6-based accelerator-in-memory supporting 1TFLOPS MAC operation and various activation functions for deep-learning applications. In *2022 IEEE International Solid-State Circuits Conference (ISSCC)*, Vol. 65. IEEE, 1–3.

[53] Sang-Won Lee, Won-Kyoung Choi, and Dong-Joo Park. 2006. FAST: An efficient flash translation layer for flash memory. In *Emerging Directions in Embedded and Ubiquitous Computing: EUC 2006 Workshops: NCUS, SecUbiqu, USN, TRUST*,

ESO, and MSA, Seoul, Korea, August 1-4, 2006. Proceedings. Springer, 879–887.

[54] Wonbeom Lee, Jungi Lee, Junghwan Seo, and Jaewoong Sim. 2024. {InfiniGen}: Efficient generative inference of large language models with dynamic {KV} cache management. In *18th USENIX Symposium on Operating Systems Design and Implementation (OSDI 24)*. 155–172.

[55] Cangyuan Li, Ying Wang, Cheng Liu, Shengwen Liang, Huawei Li, and Xiaowei Li. 2021. {GLIST}: Towards {in-storage} graph learning. In *2021 USENIX Annual Technical Conference (USENIX ATC 21)*. 225–238.

[56] Cong Li, Zhe Zhou, Sizhe Zheng, Jiaxi Zhang, Yun Liang, and Guangyu Sun. 2024. SpecPIM: Accelerating Speculative Inference on PIM-Enabled System via Architecture-Dataflow Co-Exploration. In *Proceedings of the 29th ACM International Conference on Architectural Support for Programming Languages and Operating Systems, Volume 3*. 950–965.

[57] Siqi Li, Fengbin Tu, Liu Liu, Jilan Lin, Zheng Wang, Yangwook Kang, Yufei Ding, and Yuan Xie. 2023. Ecsdd: Hardware/data layout co-designed in-storage-computing architecture for extreme classification. In *Proceedings of the 50th Annual International Symposium on Computer Architecture*. 1–14.

[58] Shengwen Liang, Ying Wang, Youyou Lu, Zhe Yang, Huawei Li, and Xiaowei Li. 2019. Cognitive {SSD}: A deep learning engine for {In-Storage} data retrieval. In *2019 USENIX Annual Technical Conference (USENIX ATC 19)*. 395–410.

[59] Akide Liu, Jing Liu, Zizheng Pan, Yefei He, Gholamreza Haffari, and Bohan Zhuang. 2024. MiniCache: KV Cache Compression in Depth Dimension for Large Language Models. *arXiv preprint arXiv:2405.14366* (2024).

[60] Lian Liu, Haimeng Ren, Long Cheng, Zhaohui Xu, Yudong Pan, Mengdi Wang, Xiaowei Li, Yinhe Han, and Ying Wang. 2024. COMET: Towards Partial W4A4KV4 LLMs Serving. *arXiv preprint arXiv:2410.12168* (2024).

[61] Yuhang Liu, Hanchen Li, Yihua Cheng, Siddhant Ray, Yuyang Huang, Qizheng Zhang, Kuntai Du, Jiayi Yao, Shan Lu, Ganesh Ananthanarayanan, et al. 2024. Cachegen: Kv cache compression and streaming for fast large language model serving. In *Proceedings of the ACM SIGCOMM 2024 Conference*. 38–56.

[62] Elliot Lockerman, Axel Feldmann, Mohammad Bakhshaliour, Alexandru Stanescu, Shashwat Gupta, Daniel Sanchez, and Nathan Beckmann. 2020. Livia: Data-centric computing throughout the memory hierarchy. In *Proceedings of the Twenty-Fifth International Conference on Architectural Support for Programming Languages and Operating Systems*. 417–433.

[63] Haocong Luo, Yahya Can Tu, F Nisa Bostancı, Ataberk Olgun, A Giray Ya, Onur Mutlu, et al. 2023. Ramulator 2.0: A Modern, Modular, and Extensible DRAM Simulator. *IEEE Computer Architecture Letters* (2023).

[64] Vikram Sharma Maiti, Zaid Qureshi, Weixin Liang, Ziyan Feng, Simon Garcia De Gonzalo, Youji Li, Hubertus Franke, Jinjun Xiong, Jian Huang, and Wen-mei Hwu. 2019. Deepstore: In-storage acceleration for intelligent queries. In *Proceedings of the 52nd Annual IEEE/ACM International Symposium on Microarchitecture*. 224–238.

[65] Nika Mansouri Ghiasi, Jisung Park, Harun Mustafa, Jeremie Kim, Ataberk Olgun, Arvid Gollwitzer, Damla Senol Cali, Can Firtina, Haiyu Mao, Nour Almadhoun Alserri, et al. 2022. GenStore: A high-performance in-storage processing system for genome sequence analysis. In *Proceedings of the 27th ACM International Conference on Architectural Support for Programming Languages and Operating Systems*. 635–654.

[66] Avinash Maurya, Jie Ye, M Mustafa Rafique, Franck Cappello, and Bogdan Nicolae. 2024. Breaking the Memory Wall: A Study of I/O Patterns and GPU Memory Utilization for Hybrid CPU-GPU Offloaded Optimizers. In *Proceedings of the 14th Workshop on AI and Scientific Computing at Scale using Flexible Computing Infrastructures*. 9–16.

[67] Microsemi Corporation. 2022. *Flashtec PCIe Gen 5 NVMe SSD Controller Evaluation Board Reference Design*. Microsemi Corporation, Aliso Viejo, CA, USA.

[68] Facebook Research Microsoft. 2017. Onnx: an open format to represent deep learning models. <https://onnx.ai/>

[69] Nandekka Nayak, Xinrui Wu, Toluwanimi O Odemuyiwa, Michael Pellauer, Joel S Emer, and Christopher W Fletcher. 2024. FuseMax: Leveraging Extended Einsums to Optimize Attention Accelerator Design. *arXiv preprint arXiv:2406.10491* (2024).

[70] Wei Niu, Jexiong Guan, Yanzhi Wang, Gagan Agrawal, and Bin Ren. 2021. Dnn-fusion: accelerating deep neural networks execution with advanced operator fusion. In *Proceedings of the 42nd ACM SIGPLAN International Conference on Programming Language Design and Implementation*. 883–898.

[71] Wei Niu, Md Musfiqur Rahman Sanim, Zhihao Shu, Jexiong Guan, Xipeng Shen, Miao Yin, Gagan Agrawal, and Bin Ren. 2024. SmartMem: Layout Transformation Elimination and Adaptation for Efficient DNN Execution on Mobile. In *Proceedings of the 29th ACM International Conference on Architectural Support for Programming Languages and Operating Systems, Volume 3*. 916–931.

[72] SiUng Noh, Junguk Hong, Chaemin Lim, Seongyeon Park, Jeehyun Kim, Hanjun Kim, Youngsok Kim, and Jinho Lee. 2024. PID-Comm: A Fast and Flexible Collective Communication Framework for Commodity Processing-in-DIMM Devices. *2024 ACM/IEEE 51st Annual International Symposium on Computer Architecture (ISCA)* (2024).

[73] NVIDIA. 2020. NVIDIA A100 Tensor Core GPU Architecture. <https://images.nvidia.com/aem-dam/en-zz/Solutions/data-center/nvidia-ampere-architecture-whitepaper.pdf>.

[74] NVIDIA. 2021. Introduction to the NVIDIA DGX A100 System. <https://docs.nvidia.com/dgx/dgxa100-user-guide/introduction-to-dgxa100.html>

[75] NVIDIA. 2022. Introduction to the NVIDIA DGX H100 System. <https://resources.nvidia.com/en-us-dgx-systems/ai-enterprise-dgx?xs=489753>

[76] NVIDIA. 2023. NVIDIA H100 Tensor Core GPU Architecture. <https://resources.nvidia.com/en-us-tensor-core/gtc22-whitepaper-hopper>

[77] OpenAI. 2023. ChatGPT. <https://chatgpt.com/blog/chatgpt>

[78] Xiupei Pan, Endian Li, Qiao Li, Shengwen Liang, Yizhou Shan, Ke Zhou, Yingwei Luo, Xiaolin Wang, and Jie Zhang. 2024. Instinfer: In-storage attention offloading for cost-effective long-context llm inference. *arXiv preprint arXiv:2409.04992* (2024).

[79] Jaehyun Park, Jaewan Choi, Kwanhee Kyung, Michael Jaemin Kim, Yongsuk Kwon, Nam Sung Kim, and Jung Ho Ahn. 2024. AttAcc! Unleashing the Power of PIM for Batched Transformer-based Generative Model Inference. In *Proceedings of the 29th ACM International Conference on Architectural Support for Programming Languages and Operating Systems, Volume 2*. 103–119.

[80] Myeong-Jae Park, Jinhung Lee, Kyungjun Cho, Jihwan Park, Junil Moon, Sung-Hak Lee, Tae-Kyun Kim, Sanghoon Oh, Seokwoo Choi, Yongsuk Choi, et al. 2022. A 192-Gb 12-high 896-GB/s HBM3 DRAM with a TSV auto-calibration scheme and machine-learning-based layout optimization. *IEEE Journal of Solid-State Circuits* 58, 1 (2022), 256–269.

[81] Sang-Soo Park, KyungSoo Kim, Jinin So, Jin Jung, Jonggeon Lee, Kyoungwan Woo, Nayeon Kim, Younghyun Lee, Hyungyo Kim, Yongsuk Kwon, et al. 2024. An LPDDR-based CXL-PNM Platform for TCO-efficient Inference of Transformer-based Large Language Models. In *2024 IEEE International Symposium on High-Performance Computer Architecture (HPCA)*. IEEE, 970–982.

[82] Pratyush Patel, Esha Choukse, Chaojie Zhang, Aashaka Shah, Íñigo Goiri, Saeed Maleki, and Ricardo Bianchini. 2024. Splitwise: Efficient generative llm inference using phase splitting. In *2024 ACM/IEEE 51st Annual International Symposium on Computer Architecture (ISCA)*. IEEE, 118–132.

[83] Cheng Peng, Xi Yang, Aokun Chen, Kaleb E Smith, Nima PourNejatian, Anthony B Costa, Cheryl Martin, Mona G Flores, Ying Zhang, Tanja Magoc, et al. 2023. A study of generative large language model for medical research and healthcare. *NPJ digital medicine* 6, 1 (2023), 210.

[84] Ramya Prabhu, Ajay Nayak, Jayashree Mohan, Ramachandran Ramjee, and Ashish Panwar. 2024. vAttention: Dynamic Memory Management for Serving LLMs without PagedAttention. *arXiv preprint arXiv:2405.04437* (2024).

[85] Ruoyu Qin, Zheming Li, Weiran He, Jialei Cui, Feng Ren, Mingxing Zhang, Yongwei Wu, Weimin Zheng, and Xinran Xu. 2025. Mooncake: Trading more storage for less computation—a KVCache-centric architecture for serving LLM chatbot. In *23rd USENIX Conference on File and Storage Technologies (FAST 25)*. USENIX Association, 155–170.

[86] Luke Ribar, Ivan Chelombiev, Luke Hudlass-Galley, Charlie Blake, Carlo Luschi, and Douglas Orr. [n. d.]. SparQ Attention: Bandwidth-Efficient LLM Inference. In *Forty-first International Conference on Machine Learning*.

[87] Baptiste Roziere, Jonas Gehring, Fabian Gloclekle, Sten Sootla, Itai Gat, Xiaojing Ellen Tan, Yossi Adi, Jingyu Liu, Romain Sauvestre, Tal Remez, et al. 2023. Code llama: Open foundation models for code. *arXiv preprint arXiv:2308.12950* (2023).

[88] SAFARI Research Group. 2023. Ramulator 2.0. <https://github.com/CMU-SAFARI/ramulator2>.

[89] Roger S Schank. 1972. Conceptual dependency: A theory of natural language understanding. *Cognitive psychology* 3, 4 (1972), 552–631.

[90] Brian C Schwedock, Piratach Yoovidhya, Jennifer Seibert, and Nathan Beckmann. 2022. Tákó: A polymorphic cache hierarchy for general-purpose optimization of data movement. In *Proceedings of the 49th Annual International Symposium on Computer Architecture*. 42–58.

[91] Samsung Semiconductor. 2018. *DDR4 Product Guide*. Technical Report. https://download.semiconductor.samsung.com/resources/product-guide/DDR4_Product_guide_18.09.pdf

[92] Minseok Seo, Xuan Truong Nguyen, Seok Joong Hwang, Yongkee Kwon, Guhyun Kim, Chanwook Park, Ilkon Kim, Jaehan Park, Jeongbin Kim, Woojae Shin, et al. 2024. JANUS: Integrated Accelerator based on NPU-PIM Unified Memory System. In *Proceedings of the 29th ACM International Conference on Architectural Support for Programming Languages and Operating Systems, Volume 3*. 545–560.

[93] Noam Shazeer. 2019. Fast transformer decoding: One write-head is all you need. *arXiv preprint arXiv:1911.02150* (2019).

[94] Zhuoran Shen, Mingyuan Zhang, Haiyu Zhao, Shuai Yi, and Hongsheng Li. 2021. Efficient attention: Attention with linear complexities. In *Proceedings of the IEEE/CVF winter conference on applications of computer vision*. 3531–3539.

[95] Ying Sheng, Lianmin Zheng, Binhang Yuan, Zhuohan Li, Max Ryabinin, Beidi Chen, Percy Liang, Christopher Ré, Ion Stoica, and Ce Zhang. 2023. Flexgen: High-throughput generative inference of large language models with a single gpu. In *International Conference on Machine Learning*. PMLR, 31094–31116.

[96] Luohu Shi, Hongyi Zhang, Yao Yao, Zuchao Li, and Hai Zhao. 2024. Keep the Cost Down: A Review on Methods to Optimize LLM’s KV-Cache Consumption. *arXiv preprint arXiv:2407.18003* (2024).

[97] Yixin Song, Zeyu Mi, Haotong Xie, and Haibo Chen. 2023. Powerinfer: Fast large language model serving with a consumer-grade gpu. *arXiv preprint arXiv:2312.12456* (2023).

[98] Synopsys. [n. d.]. Design Compiler. <http://www.synopsys.com/Tools/Implementation/RTLSynthesis/DesignCompiler/Pages>.

[99] Jiaming Tang, Yilong Zhao, Kan Zhu, Guangxuan Xiao, Baris Kasikci, and Song Han. 2024. Quest: Query-Aware Sparsity for Efficient Long-Context LLM Inference. *arXiv preprint arXiv:2406.10774* (2024).

[100] Qwen Team. 2024. Qwen2.5: A Party of Foundation Models. <https://qwenlm.github.io/blog/qwen2.5/>

[101] ShareGPT Team. 2023. ShareGPT. <https://sharegpt.com/>

[102] The Machine Learning Compilation Team. 2023. Universal LLM Deployment Engine with ML Compilation. <https://github.com/mlc-ai/mlc-llm>

[103] TenaFe. 2023. *TC2200 PCIe Gen4 NVMe DRAMless SSD Controller*. TenaFe. Available at: <https://www.tenafe.com/tc2200>.

[104] B Terry. 2022. Average reading speed (WPM) by age and grade level. *Scholar Within* (2022).

[105] the OpenSSD Team. 2024. Simulators - The OpenSSD Project. <http://www.openssd-project.org/kvssd/simulators/>

[106] Boyu Tian, Yiwei Li, Li Jiang, Shuangyu Cai, and Mingyu Gao. 2024. NDPBridge: Enabling Cross-Bank Coordination in Near-DRAM-Bank Processing Architectures. In *2024 ACM/IEEE 51st Annual International Symposium on Computer Architecture (ISCA)*. IEEE, 628–643.

[107] Hugo Touvron, Thibaut Lavril, Gautier Izacard, Xavier Martinet, Marie-Anne Lachaux, Timothée Lacroix, Baptiste Rozière, Naman Goyal, Eric Hambro, Faisal Azhar, et al. 2023. Llama: Open and efficient foundation language models. *arXiv preprint arXiv:2302.13971* (2023).

[108] Hugo Touvron, Louis Martin, Kevin Stone, Peter Albert, Amjad Almahairi, Yasmine Babaei, Nikolay Bashlykov, Soumya Batra, Prajwal Bhargava, Shruti Bhosale, et al. 2023. Llama 2: Open foundation and fine-tuned chat models. *arXiv preprint arXiv:2307.09288* (2023).

[109] Tri, Dao and Daniel, Haziza and Francisco, Massa and Grigory, Sizov. 2023. Flash-Decoding for long-context inference. <https://pytorch.org/blog/flash-decoding>.

[110] A Vaswani. 2017. Attention is all you need. *Advances in Neural Information Processing Systems* (2017).

[111] Zhengrong Wang, Christopher Liu, Nathan Beckmann, and Tony Nowatzki. 2023. Affinity Alloc: Taming Not-So-Near-Data Computing. In *Proceedings of the 56th Annual IEEE/ACM International Symposium on Microarchitecture*. 784–799.

[112] Jason Wei, Xuezhi Wang, Dale Schuurmans, Maarten Bosma, Fei Xia, Ed Chi, Quoc V Le, Denny Zhou, et al. 2022. Chain-of-thought prompting elicits reasoning in large language models. *Advances in neural information processing systems* 35 (2022), 24824–24837.

[113] Mark Wilkening, Udit Gupta, Samuel Hsia, Caroline Trippel, Carole-Jean Wu, David Brooks, and Gu-Yeon Wei. [n. d.]. RecSSD: Near Data Processing for Solid State Drive Based Recommendation Inference Extended Abstract. ([n. d.]).

[114] Bingyang Wu, Shengyu Liu, Yinmin Zhong, Peng Sun, Xuanzhe Liu, and Xin Jin. 2024. Loongserve: Efficiently serving long-context large language models with elastic sequence parallelism. In *Proceedings of the ACM SIGOPS 30th Symposium on Operating Systems Principles*. 640–654.

[115] Kan Wu, Zhihan Guo, Guanzhou Hu, Kaiwei Tu, Ramnaththan Alagappan, Rathijit Sen, Kwanghyun Park, Andrea C Arpacı-Dusseau, and Remzi H Arpacı-Dusseau. 2021. The storage hierarchy is not a hierarchy: Optimizing caching on modern storage devices with orthus. In *19th USENIX Conference on File and Storage Technologies (FAST 21)*. 307–323.

[116] Yuting Wu, Ziye Wang, and Wei D Lu. 2024. PIM GPT a hybrid process in memory accelerator for autoregressive transformers. *npj Unconventional Computing* 1, 1 (2024), 4.

[117] Guangxuan Xiao, Jiaming Tang, Jingwei Zuo, Junxian Guo, Shang Yang, Haotian Tang, Yao Fu, and Song Han. 2024. DuoAttention: Efficient Long-Context LLM Inference with Retrieval and Streaming Heads. *arXiv preprint arXiv:2410.10819* (2024).

[118] Yao Xiao, Shahin Nazarian, and Paul Bogdan. 2018. Prometheus: Processing-in-memory heterogeneous architecture design from a multi-layer network theoretic strategy. In *2018 Design, Automation & Test in Europe Conference & Exhibition (DATE)*. IEEE, 1387–1392.

[119] Haoyi Xiong, Jiang Bian, Yuchen Li, Xuhong Li, Mengnan Du, Shuaiqiang Wang, Dawei Yin, and Sumi Helal. 2024. When search engine services meet large language models: visions and challenges. *IEEE Transactions on Services Computing* (2024).

[120] Jiale Xu, Rui Zhang, Cong Guo, Weiming Hu, Zihan Liu, Feiyang Wu, Yu Feng, Shixuan Sun, Changxu Shao, Yuhong Guo, et al. 2024. vTensor: Flexible Virtual Tensor Management for Efficient LLM Serving. *arXiv preprint arXiv:2407.15309* (2024).

[121] Zhenliang Xue, Yixin Song, Zeyu Mi, Le Chen, Yubin Xia, and Haibo Chen. 2024. PowerInfer-2: Fast Large Language Model Inference on a Smartphone. *arXiv preprint arXiv:2406.06282* (2024).

[122] Juncheng Yang, Yazhuo Zhang, Ziyue Qiu, Yao Yue, and Rashmi Vinayak. 2023. FIFO queues are all you need for cache eviction. In *Proceedings of the 29th Symposium on Operating Systems Principles*. 130–149.

[123] Shuo Yang, Ying Sheng, Joseph E Gonzalez, Ion Stoica, and Lianmin Zheng. 2024. Post-Training Sparse Attention with Double Sparsity. *arXiv preprint arXiv:2408.07092* (2024).

[124] Tzu-Wei Yang, Seth Pollen, Mustafa Uysal, Arif Merchant, and Homer Wolfmeyer. 2022. {CacheSack}: Admission Optimization for Google Datacenter Flash Caches. In *2022 USENIX Annual Technical Conference (USENIX ATC 22)*. 1021–1036.

[125] Shunyu Yao, Dian Yu, Jeffrey Zhao, Izhak Shafran, Tom Griffiths, Yuan Cao, and Karthik Narasimhan. 2024. Tree of thoughts: Deliberate problem solving with large language models. *Advances in Neural Information Processing Systems* 36 (2024).

[126] Gyeong-In Yu, Joo Seong Jeong, Geon-Woo Kim, Soojeong Kim, and Byung-Gon Chun. 2022. Orca: A distributed serving system for {Transformer-Based} generative models. In *16th USENIX Symposium on Operating Systems Design and Implementation (OSDI 22)*. 521–538.

[127] Zhongkai Yu, Shengwen Liang, Tianyuan Ma, Yunke Cai, Ziyuan Nan, Di Huang, Xinkai Song, Yifan Hao, Jie Zhang, Tian Zhi, et al. 2024. Cambricon-llm: A chiplet-based hybrid architecture for on-device inference of 70b llm. *arXiv preprint arXiv:2409.15654* (2024).

[128] Mohamed Zahran. 2007. Cache replacement policy revisited. *WDDD held in conjunction with ISCA* (2007), 1–8.

[129] Hailin Zhang, Xiaodong Ji, Yilin Chen, Fangcheng Fu, Xupeng Miao, Xiaonan Nie, Weipeng Chen, and Bin Cui. 2024. PQCache: Product Quantization-based KVCache for Long Context LLM Inference. *CoRR* (2024).

[130] Hengrui Zhang, August Ning, Rohan Baskar Prabhakar, and David Wentzlaff. 2024. Llmcompass: Enabling efficient hardware design for large language model inference. In *2024 ACM/IEEE 51st Annual International Symposium on Computer Architecture (ISCA)*. IEEE, 1080–1096.

[131] Susan Zhang, Stephen Roller, Naman Goyal, Mikel Artetxe, Moya Chen, Shuhui Chen, Christopher Dewan, Mona Diab, Xian Li, Xi Victoria Lin, et al. 2022. Opt: Open pre-trained transformer language models. *arXiv preprint arXiv:2205.01068* (2022).

[132] Yuxin Zhang, Yuxuan Du, Gen Luo, Yunshan Zhong, Zhenyu Zhang, Shiwei Liu, and Rongrong Ji. 2024. CaM: Cache Merging for Memory-efficient LLMs Inference. In *Forty-first International Conference on Machine Learning*.

[133] Zhenyu Zhang, Ying Sheng, Tianyi Zhou, Tianlong Chen, Lianmin Zheng, Ruisi Cai, Zhao Song, Yuandong Tian, Christopher Ré, Clark Barrett, et al. 2023. H2o: Heavy-hitter oracle for efficient generative inference of large language models. *Advances in Neural Information Processing Systems* 36 (2023), 34661–34710.

[134] Wenting Zhao, Xiang Ren, Jack Hessel, Claire Cardie, Yebin Choi, and Yuntian Deng. 2024. Wildchat: 1m chatGPT interaction logs in the wild. *arXiv preprint arXiv:2405.01470* (2024).

[135] Yilong Zhao, Mingyu Gao, Fangxin Liu, Yiwei Hu, Zongwu Wang, Han Lin, Ji Li, He Xian, Hanlin Dong, Tao Yang, et al. 2024. UM-PIM: DRAM-based PIM with Uniform & Shared Memory Space. In *2024 ACM/IEEE 51st Annual International Symposium on Computer Architecture (ISCA)*. IEEE, 644–659.

[136] Liyan Zheng, Haojie Wang, Jidong Zhai, Muyan Hu, Zixuan Ma, Tuowei Wang, Shuhong Huang, Xupeng Miao, Shizhi Tang, Kezhao Huang, et al. 2023. {EINNET}: Optimizing tensor programs with {Derivation-Based} transformations. In *17th USENIX Symposium on Operating Systems Design and Implementation (OSDI 23)*. 739–755.

[137] Size Zheng, Siyuan Chen, Peidi Song, Renze Chen, Xiuhong Li, Shengen Yan, Dahua Lin, Jingwen Leng, and Yun Liang. 2023. Chimera: An analytical optimizing framework for effective compute-intensive operators fusion. In *2023 IEEE International Symposium on High-Performance Computer Architecture (HPCA)*. IEEE, 1113–1126.

[138] Yinnin Zhong, Shengyu Liu, Junda Chen, Jianbo Hu, Yibo Zhu, Xuanzhe Liu, Xin Jin, and Hao Zhang. 2024. {DistServe}: Disaggregating Prefill and Decoding for Goodput-optimized Large Language Model Serving. In *18th USENIX Symposium on Operating Systems Design and Implementation (OSDI 24)*. 193–210.

[139] Minxuan Zhou, Weihong Xu, Jaeyoung Kang, and Tajana Rosing. 2022. Transpim: A memory-based acceleration via software-hardware co-design for transformer. In *2022 IEEE International Symposium on High-Performance Computer Architecture (HPCA)*. IEEE, 1071–1085.

[140] Zhe Zhou, Cong Li, Fan Yang, and Guangyu Sun. 2023. Dimm-link: Enabling efficient inter-dimm communication for near-memory processing. In *2023 IEEE International Symposium on High-Performance Computer Architecture (HPCA)*. IEEE, 302–316.